

Electronic Supplementary Information

Synthesis of New Acyclic Chelators H₄aPyta and H₆aPyha and their Complexes with Cu²⁺, Ga³⁺, Y³⁺, and Bi³⁺

Anastasia D. Zubenko, Anna A. Shchukina, Ekaterina Y. Chernikova, Bayirta V. Egorova, Irina S. Ikonnikova, Anna B. Priselkova, Anton A. Larenkov, Viktor B. Bubenshchikov, Artem A. Mitrofanov, Yury V. Fedorov, Olga A. Fedorova

Content

1. NMR and mass spectra of compounds.....	2
2. Mass spectra of complexes	12
3. NMR study of ligand protonation and complex formation.....	16
4. HPLC of complexes	18
5. DFT calculations	22
6. Radiolabeling.....	25
7. <i>In vitro</i> stability.....	27
8. Potentiometry	28

1. NMR and mass spectra of compounds

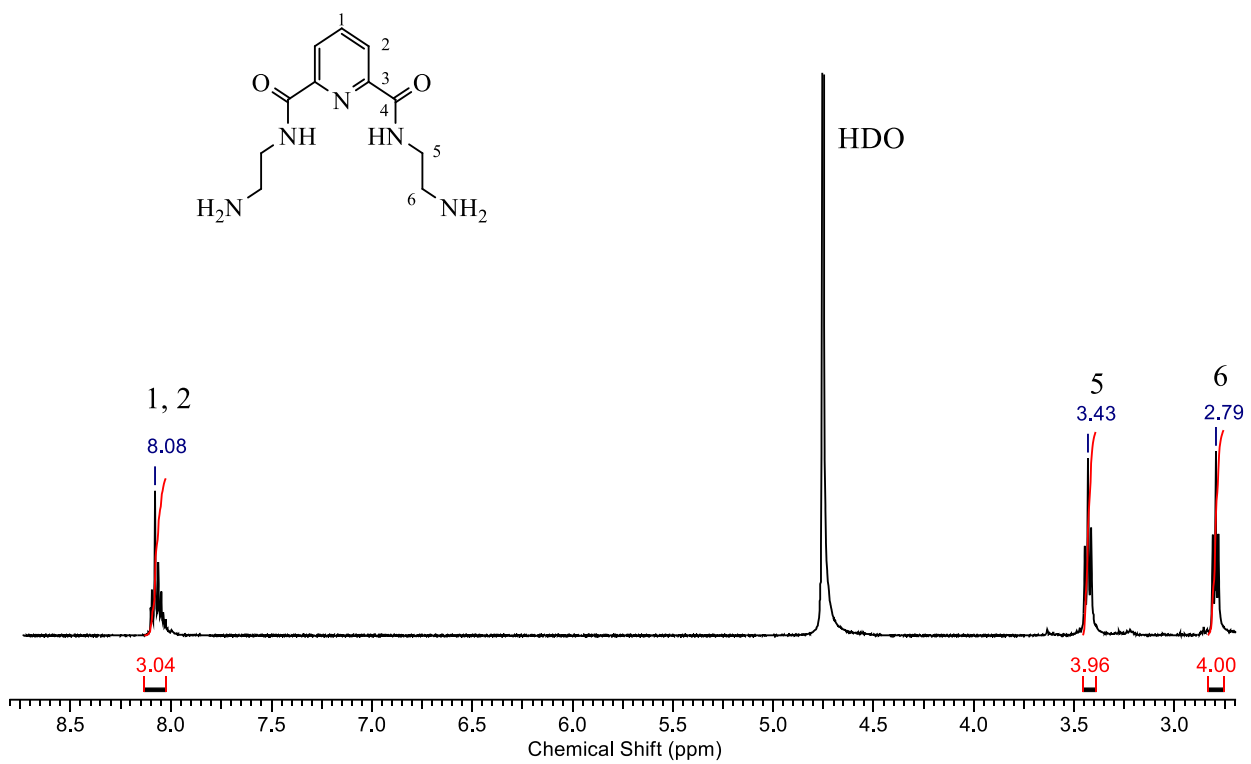


Figure S1. ^1H NMR spectrum of **2** in D_2O .

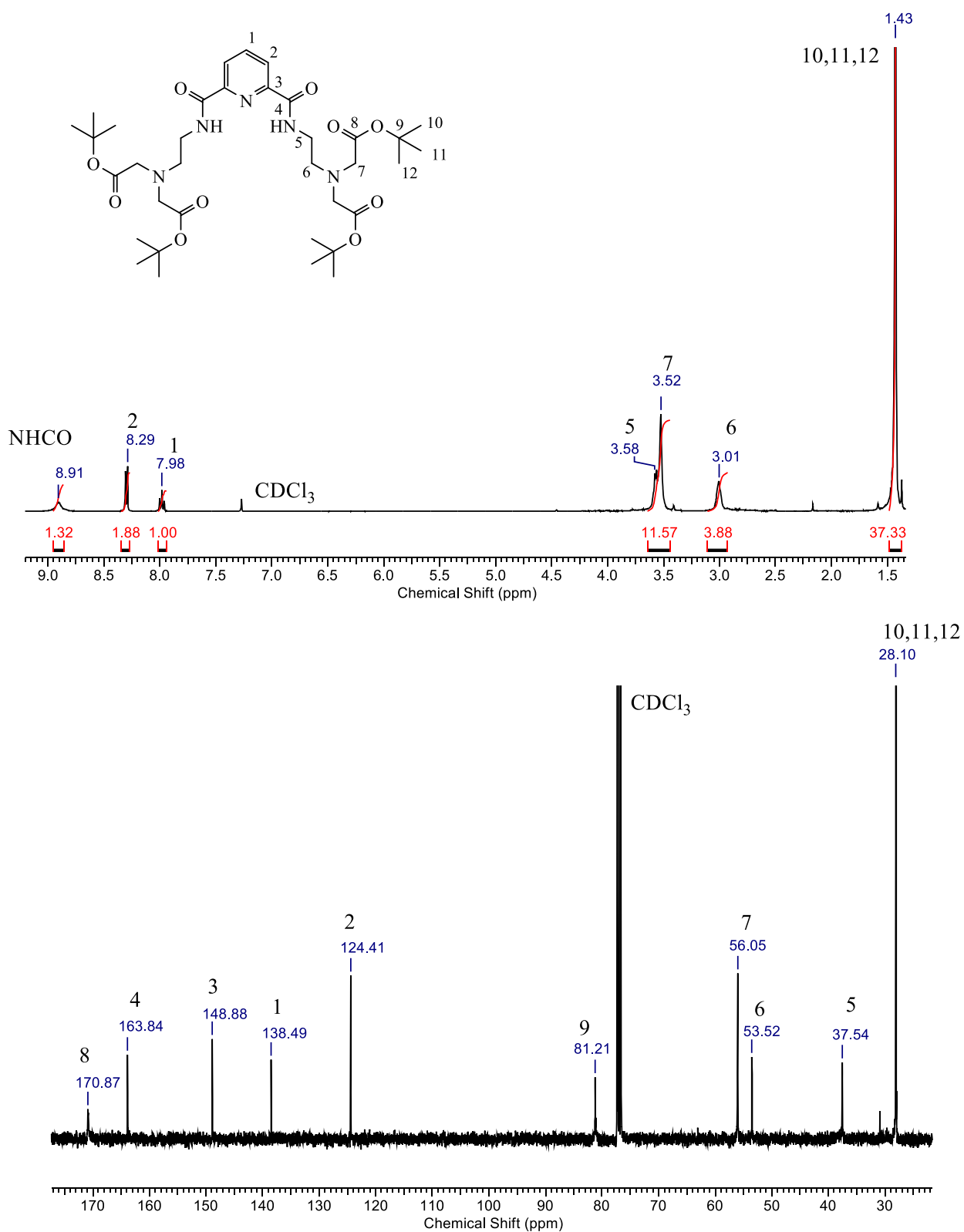


Figure S2. ¹H and ¹³C NMR spectra of **3** in CDCl₃.

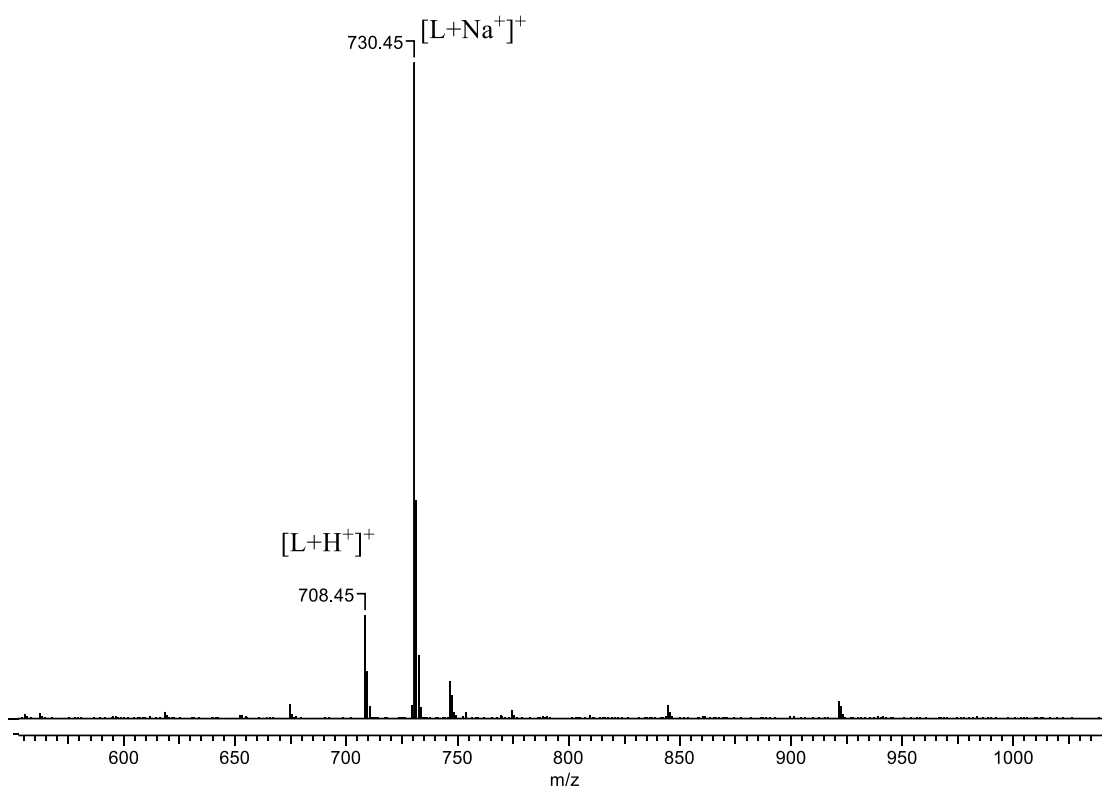


Figure S3. MS (ESI) spectrum of **3**.

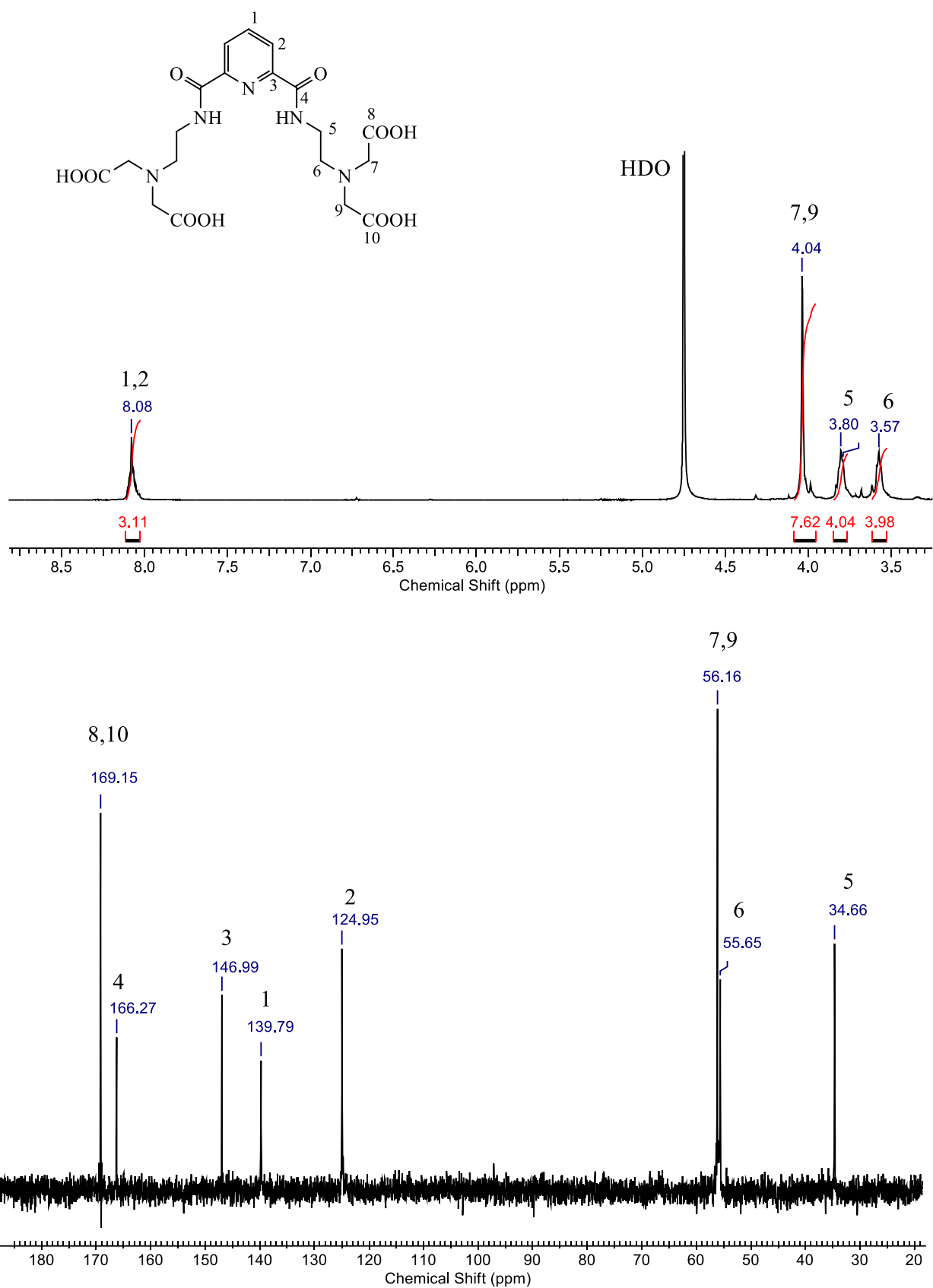


Figure S4. ¹H and ¹³C NMR spectra of H₄aPyta in D₂O.

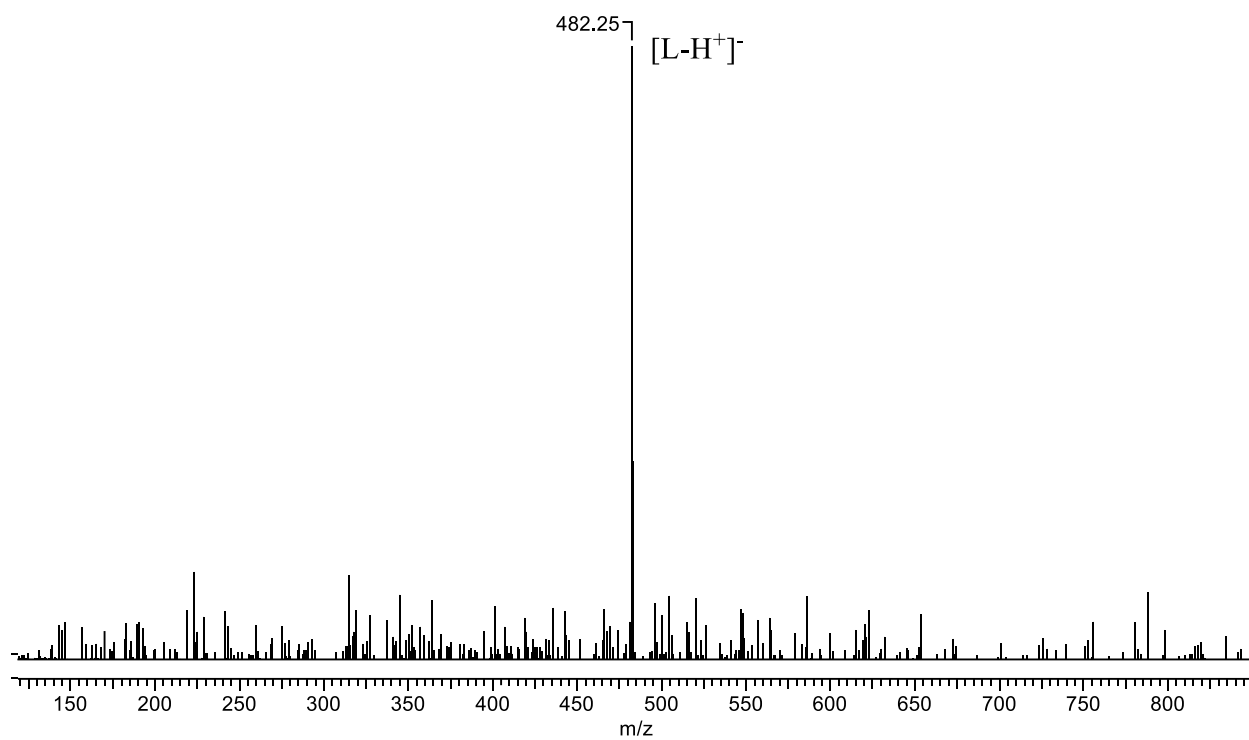


Figure S5. MS (ESI) spectrum of H₄aPyta.

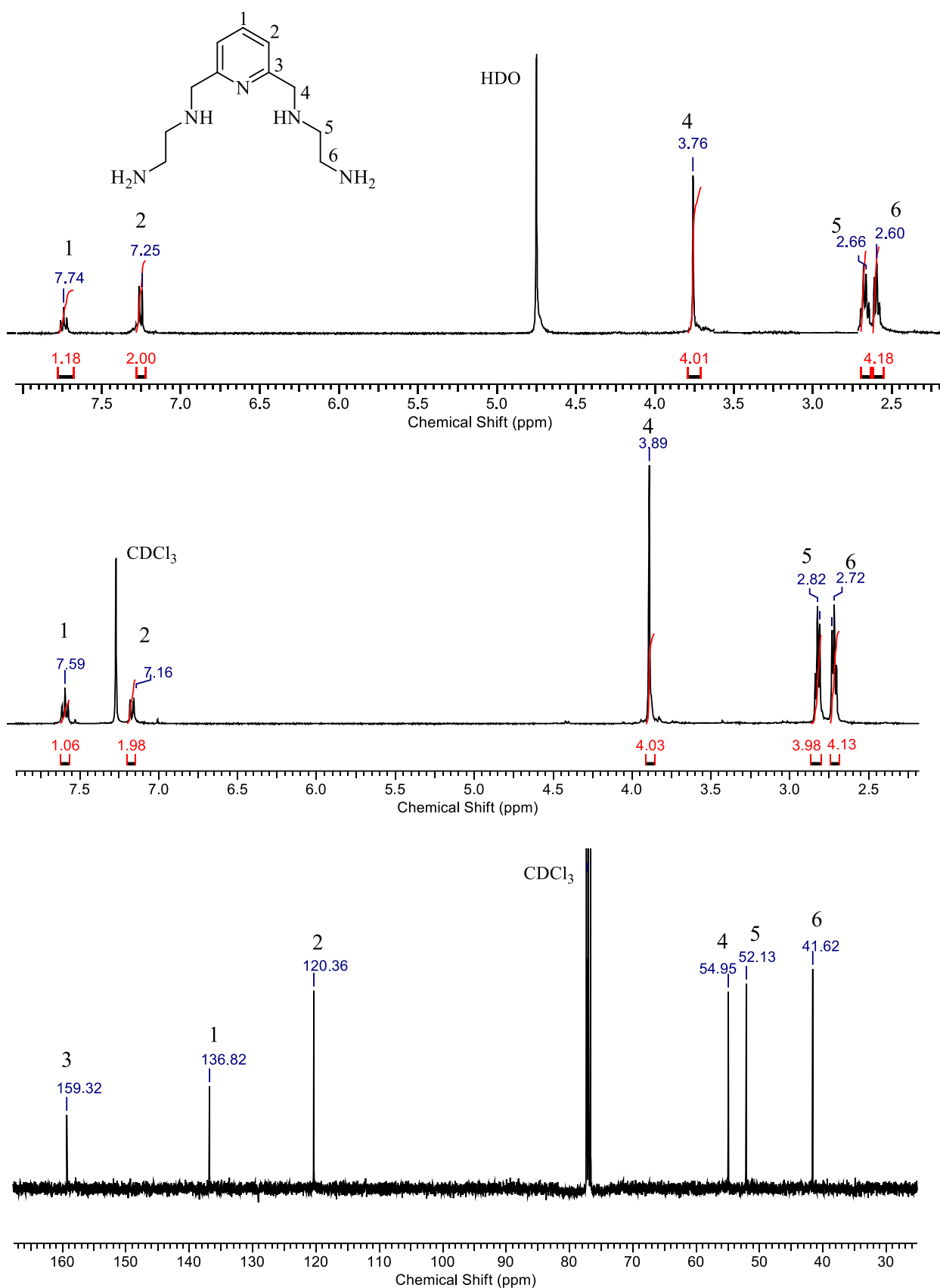


Figure S6. ^1H and ^{13}C NMR spectra of **5** in D_2O and CDCl_3 .

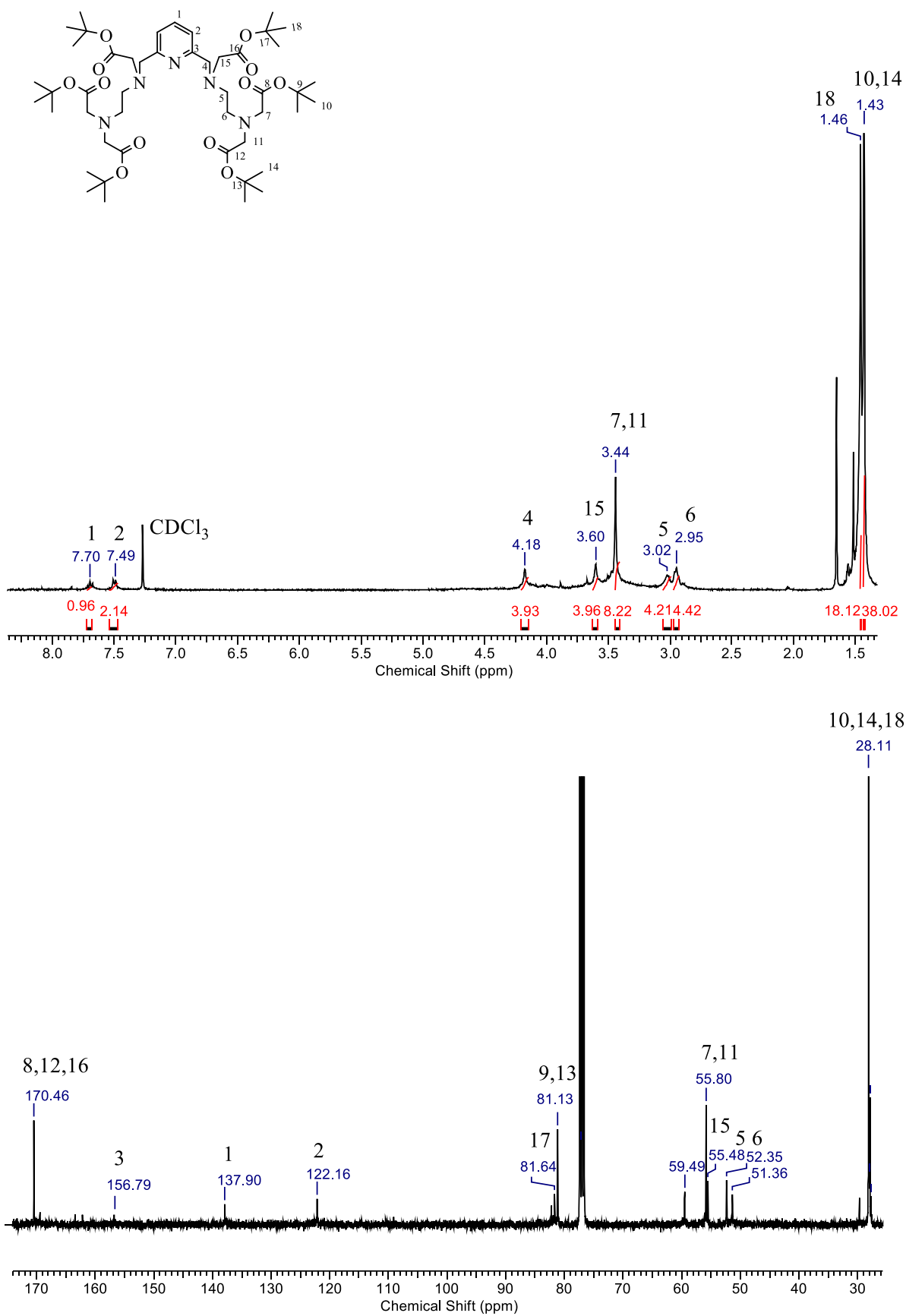


Figure S7. ¹H and ¹³C NMR spectra of **6** in CDCl₃.

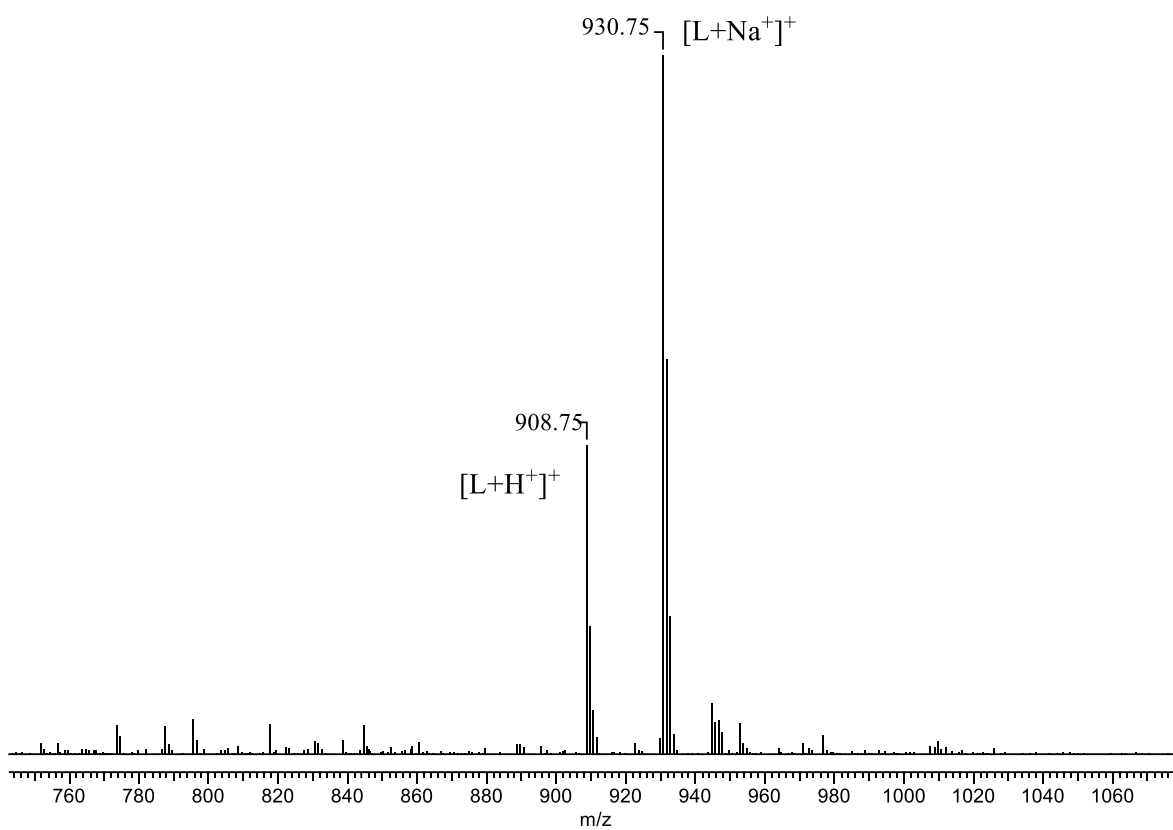


Figure S8. MS (ESI) spectrum of **6**.

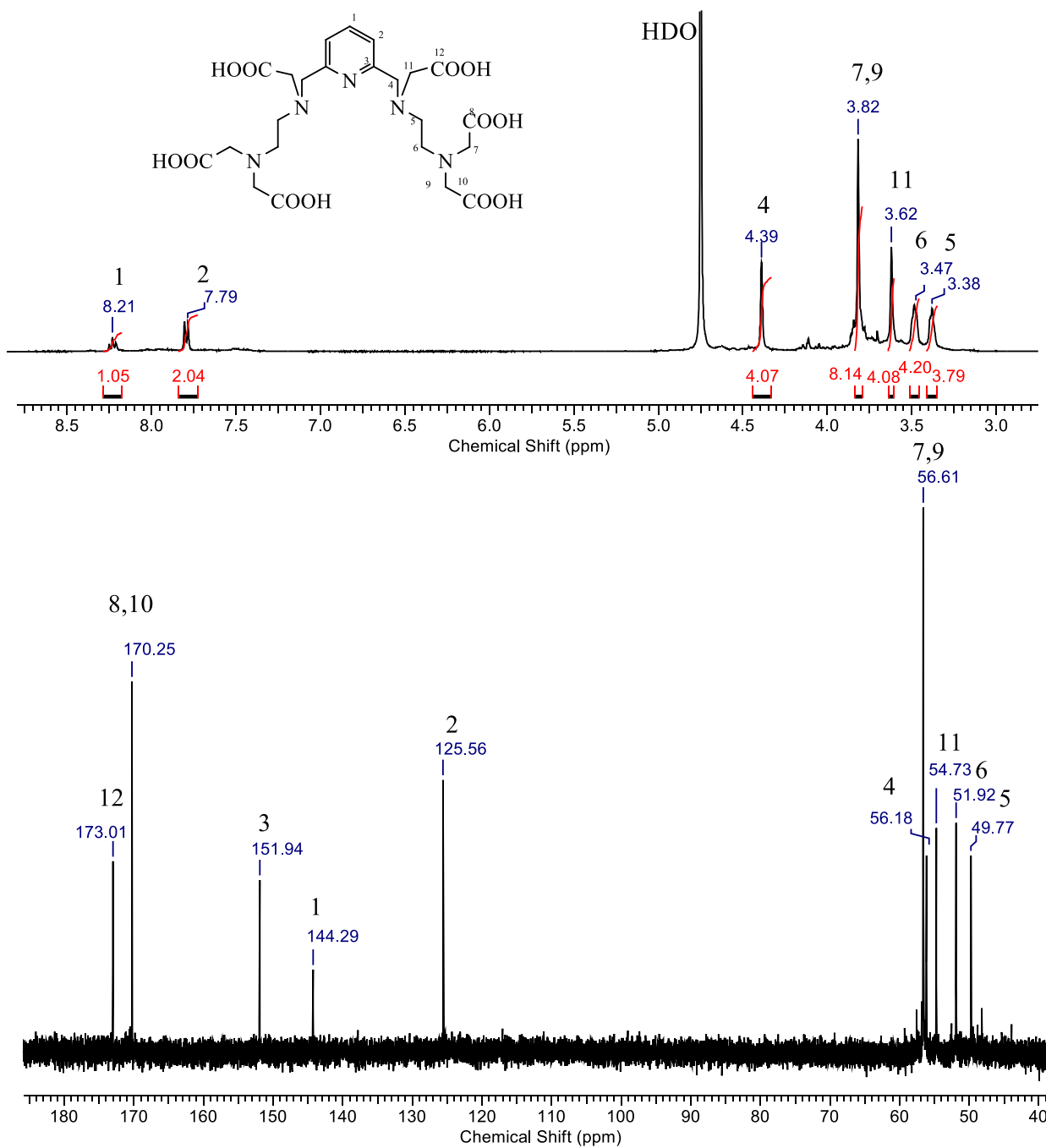


Figure S9. ¹H and ¹³C NMR spectra of H₆aPyha in D₂O.

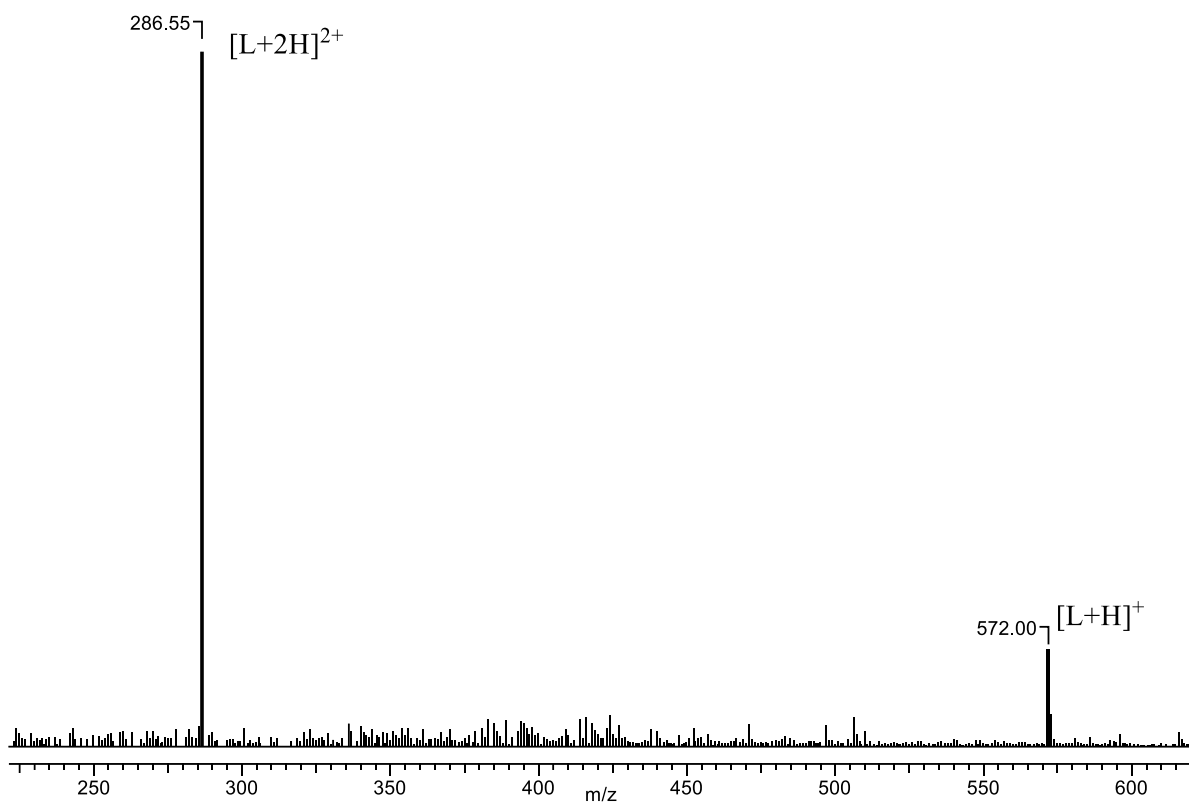


Figure S10. MS (ESI) spectrum of **H_{6a}Pyha**.

2. Mass spectra of complexes

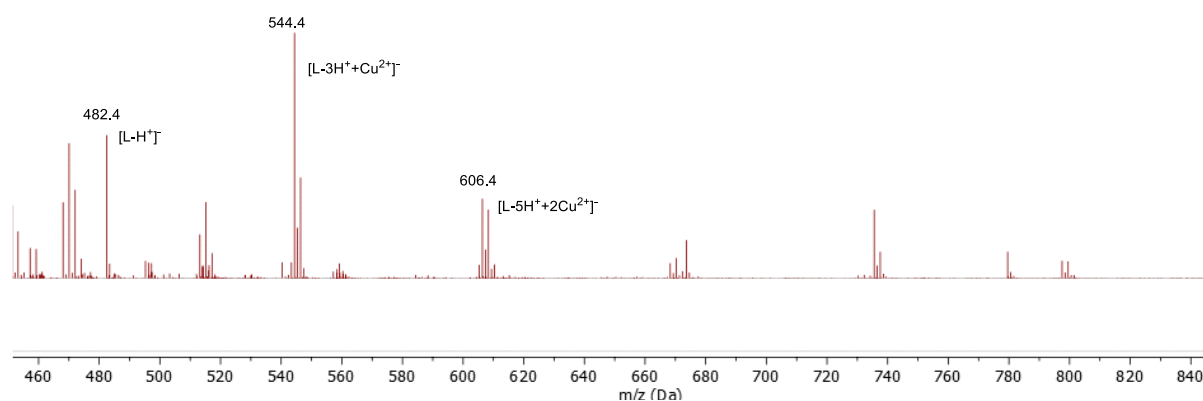


Fig. S11 MS (MALDI TOF) spectra of the ligand **H₄aPyta** in the presence of Cu²⁺.

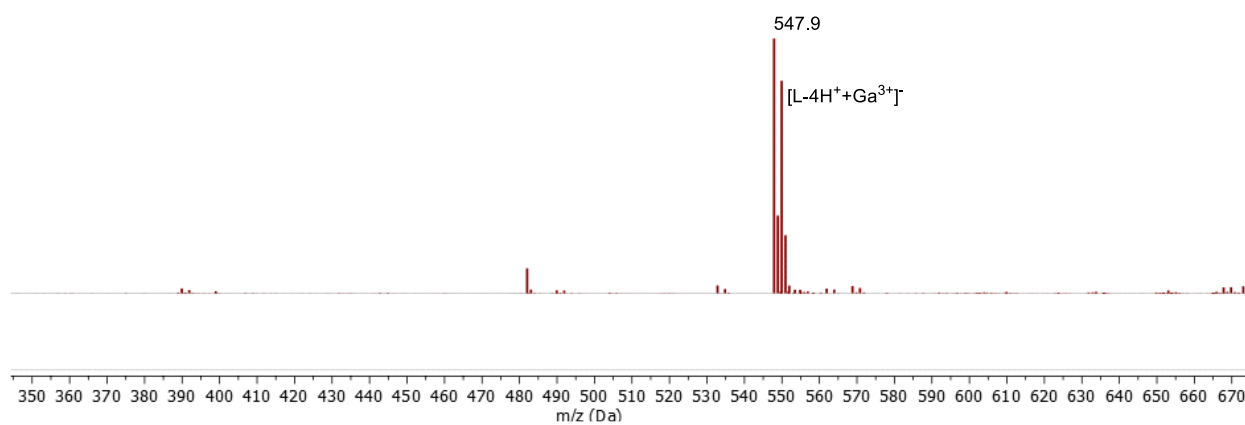


Fig. S12 MS (MALDI TOF) spectrum of the ligand **H₄aPyta** in the presence of Ga³⁺.

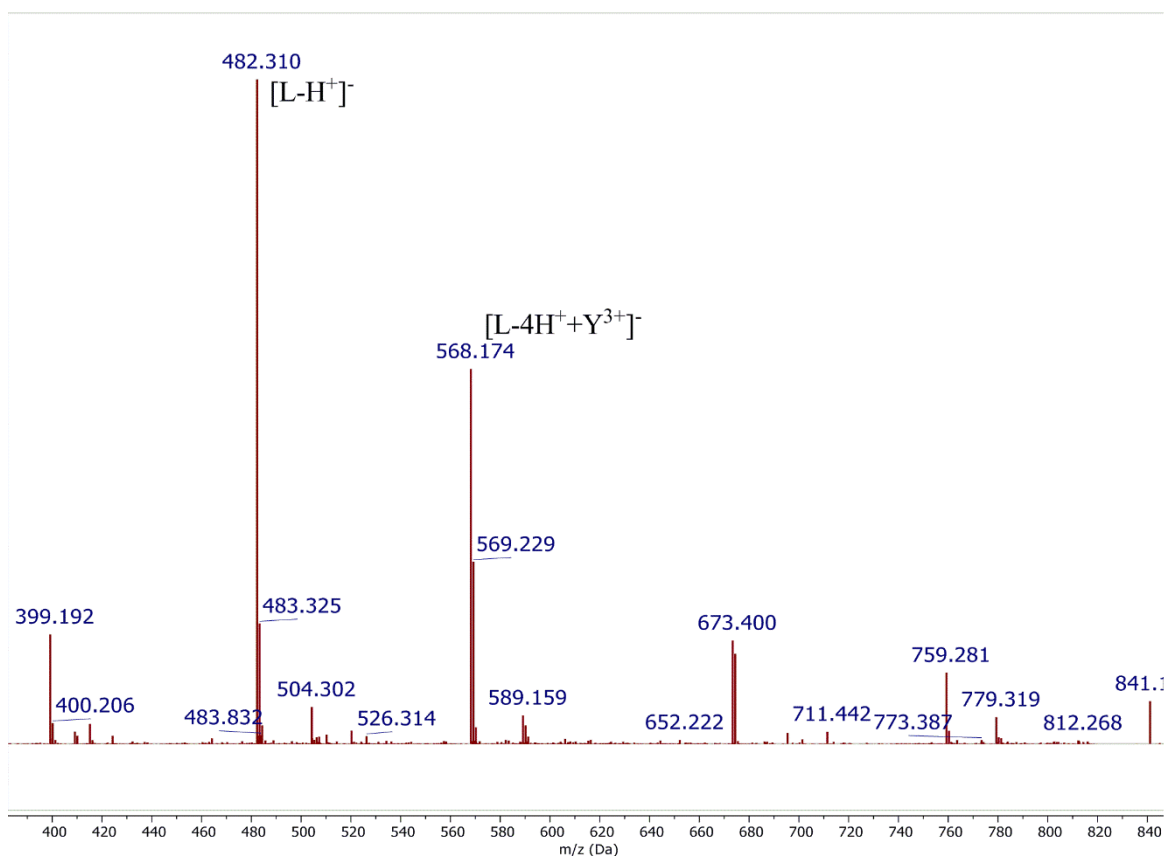


Figure S13. MS (MALDI TOF) spectrum of the ligand **H_{4a}Pyta** in the presence of **Y³⁺**.

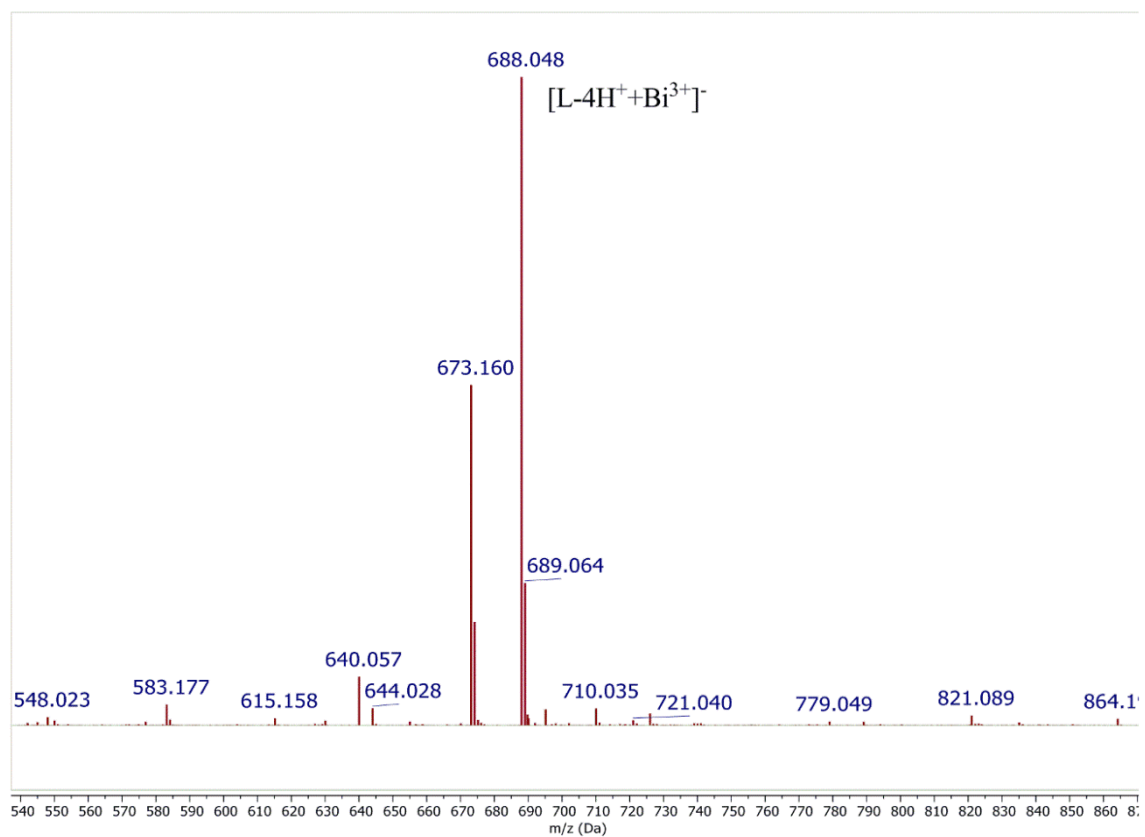


Figure S14. MS (MALDI TOF) spectrum of the ligand **H_{4a}Pyta** in the presence of **Bi³⁺**.

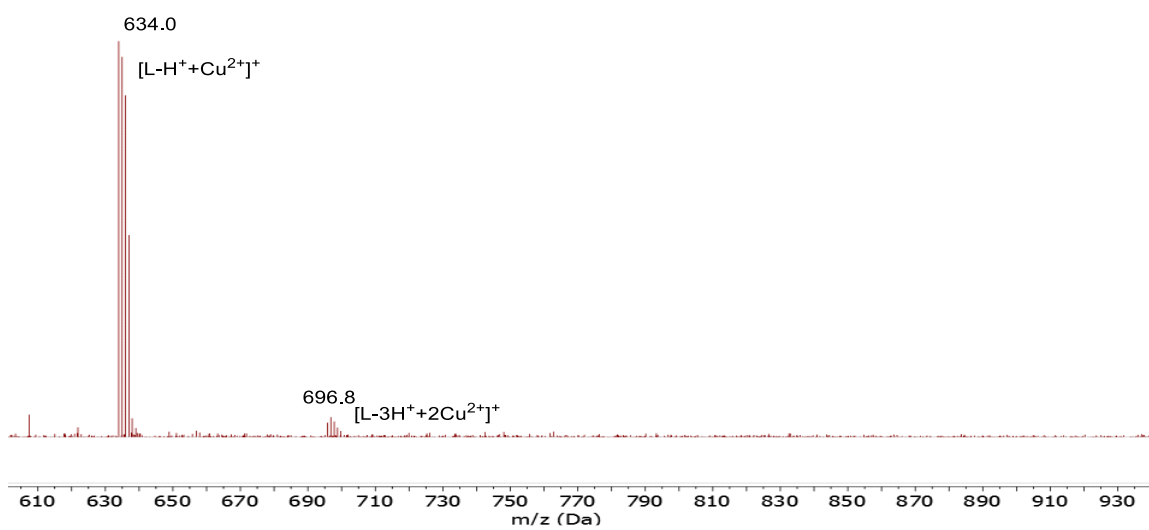


Fig. S15 MS (MALDI TOF) spectra of the ligand **H_{6a}Pyha** in the presence of Cu²⁺.

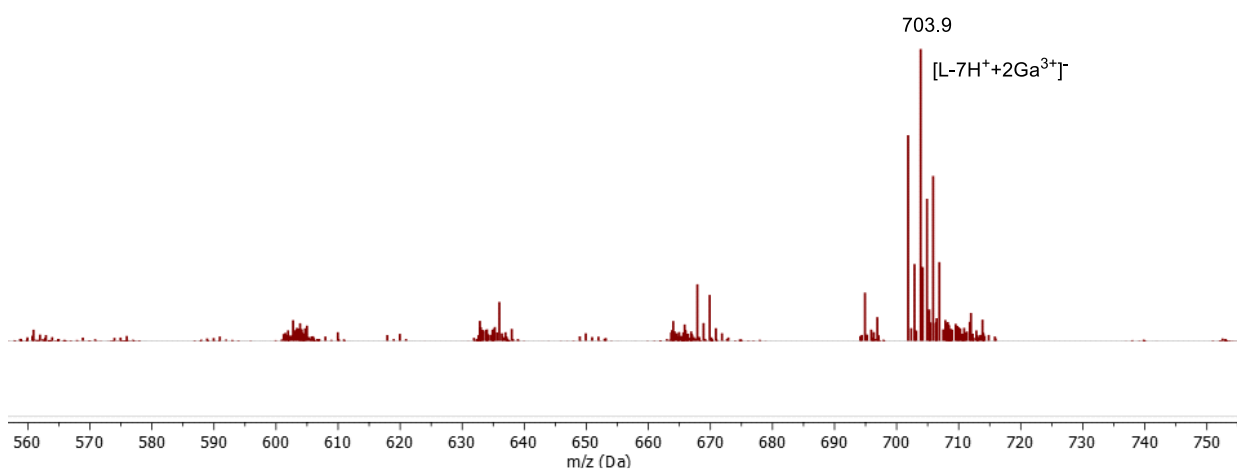


Fig. S16 MS (MALDI TOF) spectrum of the ligand **H_{6a}Pyha** in the presence of Ga³⁺.

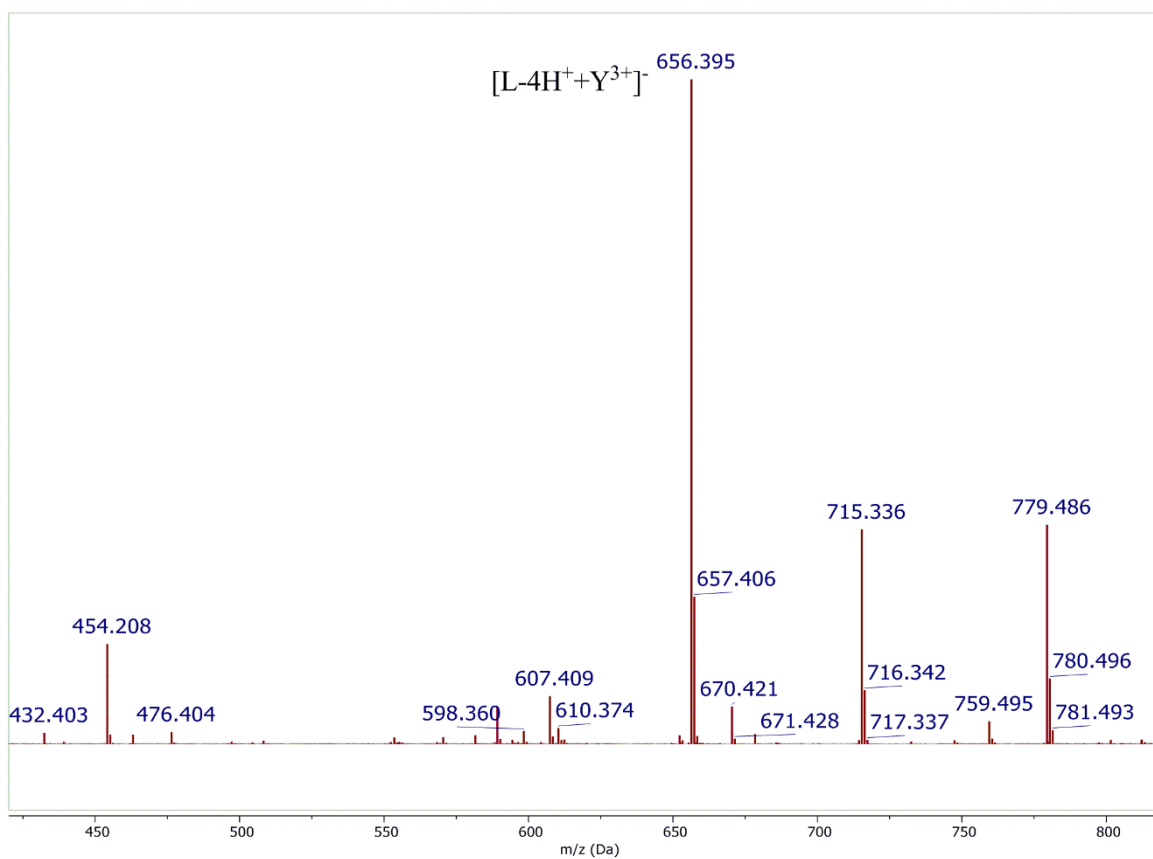


Figure S17. MS (MALDI TOF) spectrum of the ligand H_6aPyha in the presence of Y^{3+} .

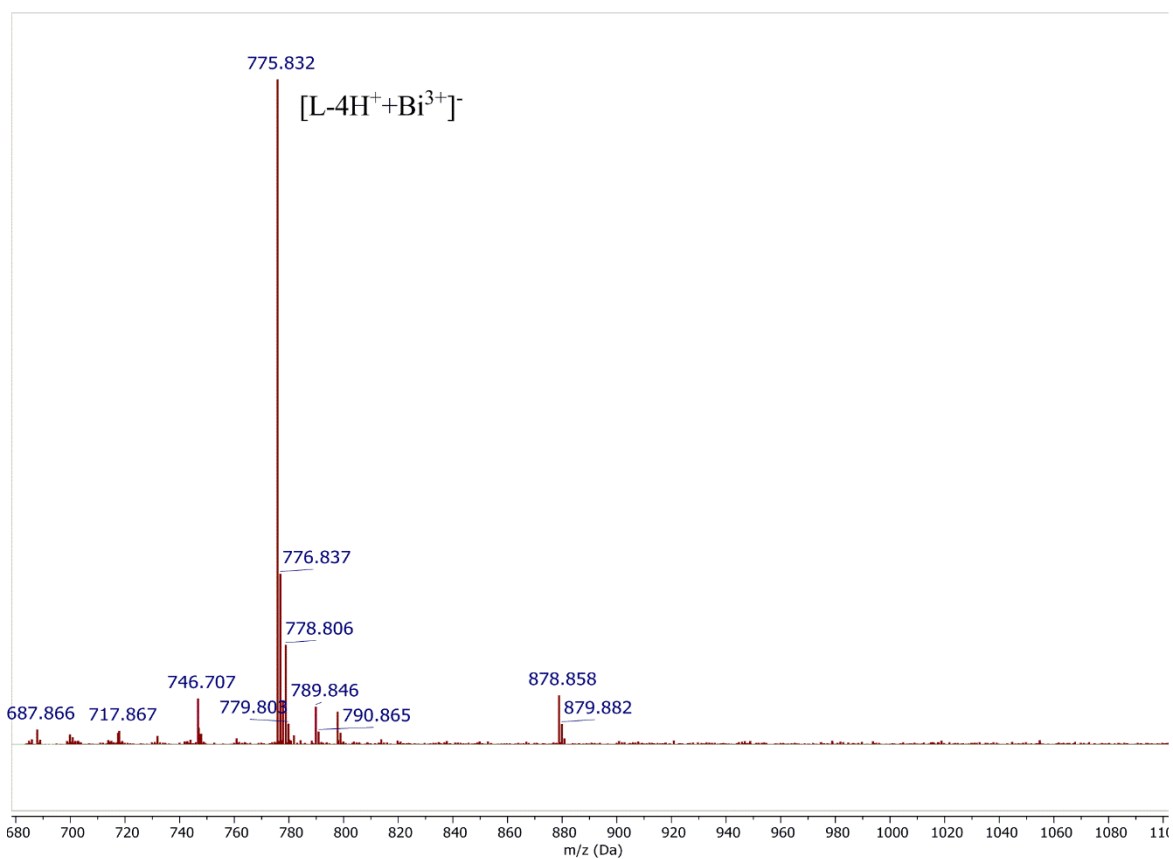


Figure S18. MS (MALDI TOF) spectrum of the ligand H_6aPyha in the presence of Bi^{3+} .

3. NMR study of ligand protonation and complex formation

Table S1. ^1H NMR (400 MHz, 298 K) chemical shifts ($\Delta\delta$, ppm) of the ligand **H₄aPyta** at different pH values in D₂O. See Figure 2 for proton labeling.

H ₄ aPyta	pH			
	12	8.7	7.3	2.2
H ₁	8.09	8.11 ($\Delta\delta = 0.02$)	8.14 ($\Delta\delta = 0.05$)	8.15 ($\Delta\delta = 0.06$)
H ₂	8.14	8.17 ($\Delta\delta = 0.03$)	8.18 ($\Delta\delta = 0.04$)	8.19 ($\Delta\delta = 0.05$)
H ₅	3.47	3.66 ($\Delta\delta = 0.19$)	3.84 ($\Delta\delta = 0.37$)	3.87 ($\Delta\delta = 0.40$)
H ₆	2.82	3.24 ($\Delta\delta = 0.42$)	3.54 ($\Delta\delta = 0.74$)	3.62 ($\Delta\delta = 0.80$)
H _{7,9}	3.24	3.59 ($\Delta\delta = 0.35$)	3.84 ($\Delta\delta = 0.60$)	4.04 ($\Delta\delta = 0.80$)

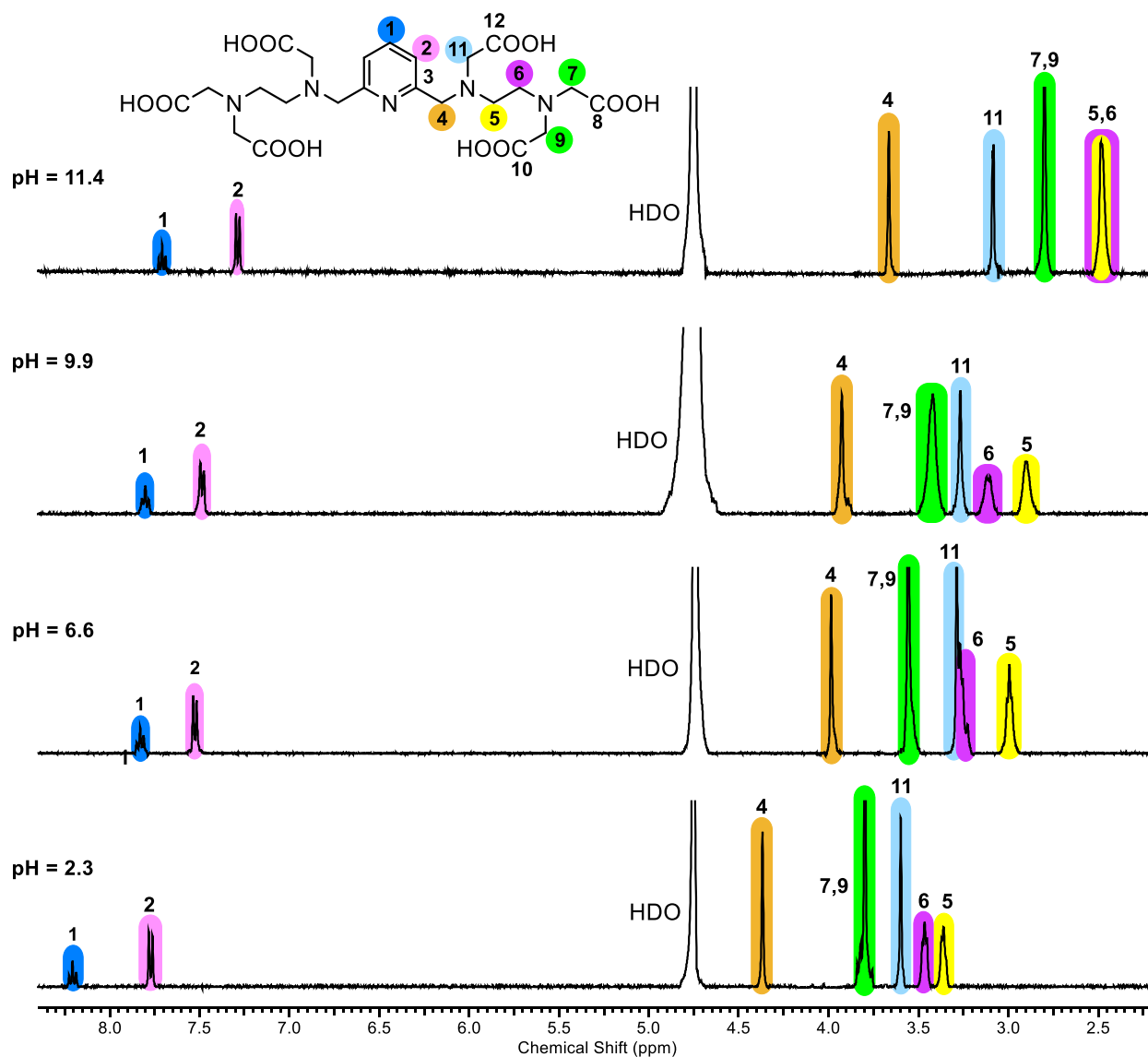


Figure S19. ^1H NMR spectra of the ligand **H₆aPyha** ($C_L = 15$ mM) at different pH values in D₂O.

Table S2. ^1H NMR (400 MHz, 298 K) chemical shifts ($\Delta\delta$, ppm) of the ligand **H_{6a}Pyha** at different pH values in D₂O. See Figure S19 for proton labeling.

H _{6a} Pyha	pH			
	11.4	9.9	6.6	2.3
H ₁	7.71	7.80 ($\Delta\delta = 0.09$)	7.83 ($\Delta\delta = 0.12$)	8.21 ($\Delta\delta = 0.50$)
H ₂	7.28	7.48 ($\Delta\delta = 0.20$)	7.52 ($\Delta\delta = 0.24$)	7.76 ($\Delta\delta = 0.48$)
H ₄	3.66	3.93 ($\Delta\delta = 0.27$)	3.99 ($\Delta\delta = 0.33$)	4.37 ($\Delta\delta = 0.71$)
H ₅	2.48	2.90 ($\Delta\delta = 0.42$)	2.99 ($\Delta\delta = 0.51$)	3.36 ($\Delta\delta = 0.88$)
H ₆	2.48	3.11 ($\Delta\delta = 0.63$)	3.25 ($\Delta\delta = 0.77$)	3.47 ($\Delta\delta = 0.99$)
H _{7,9}	2.80	3.42 ($\Delta\delta = 0.62$)	3.56 ($\Delta\delta = 0.76$)	3.80 ($\Delta\delta = 1.00$)
H ₁₁	3.08	3.27 ($\Delta\delta = 0.19$)	3.29 ($\Delta\delta = 0.21$)	3.60 ($\Delta\delta = 0.52$)

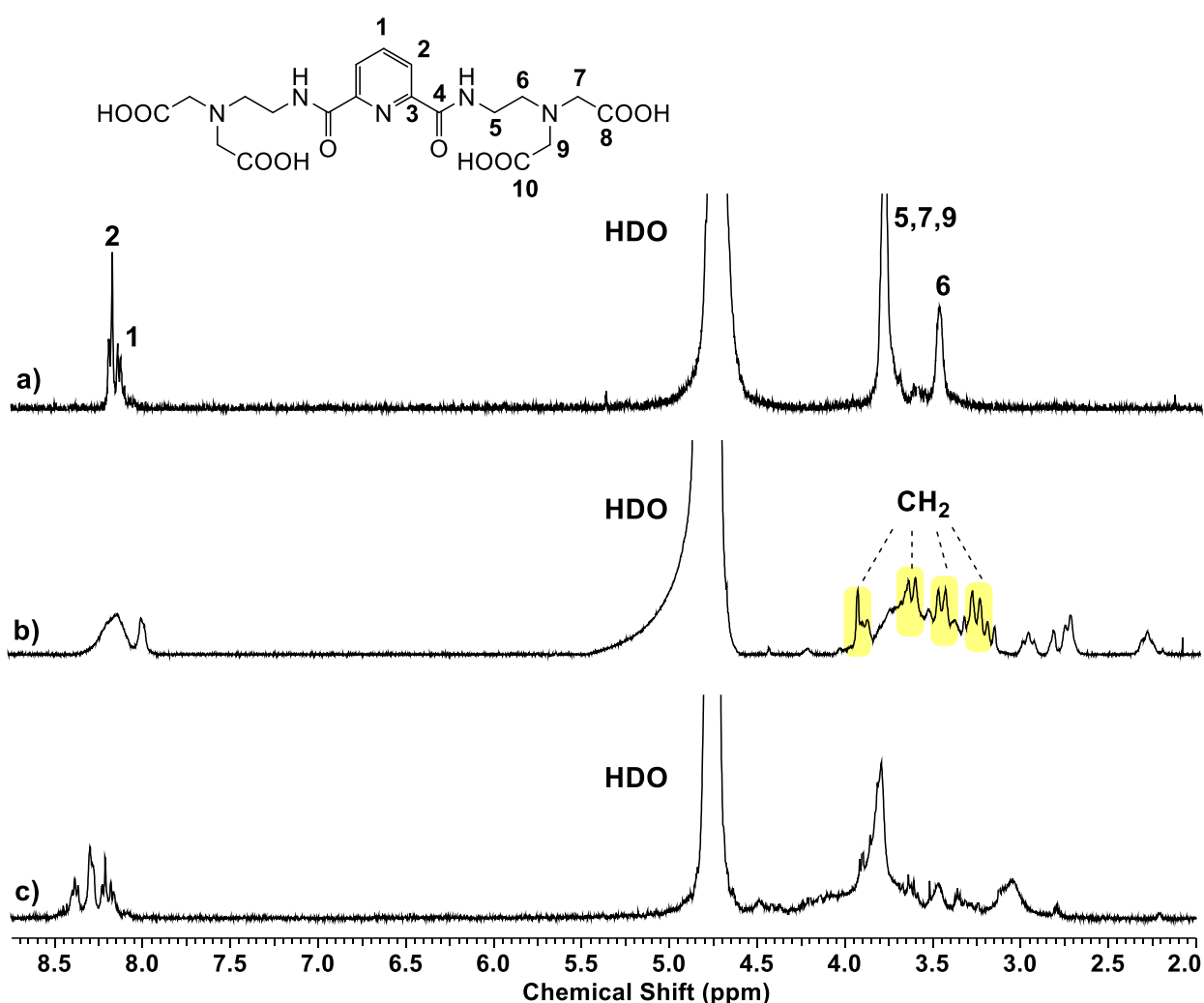


Figure S20. ^1H NMR spectra of: a) **H_{4a}Pyta** ($C_L = 10$ mM, pH=7.1), b) **H_{4a}Pyta** in the presence of Y^{3+} (pH=7.2), c) **H_{4a}Pyta** in the presence of Bi^{3+} (pH=7.5) in D₂O.

4. HPLC of complexes

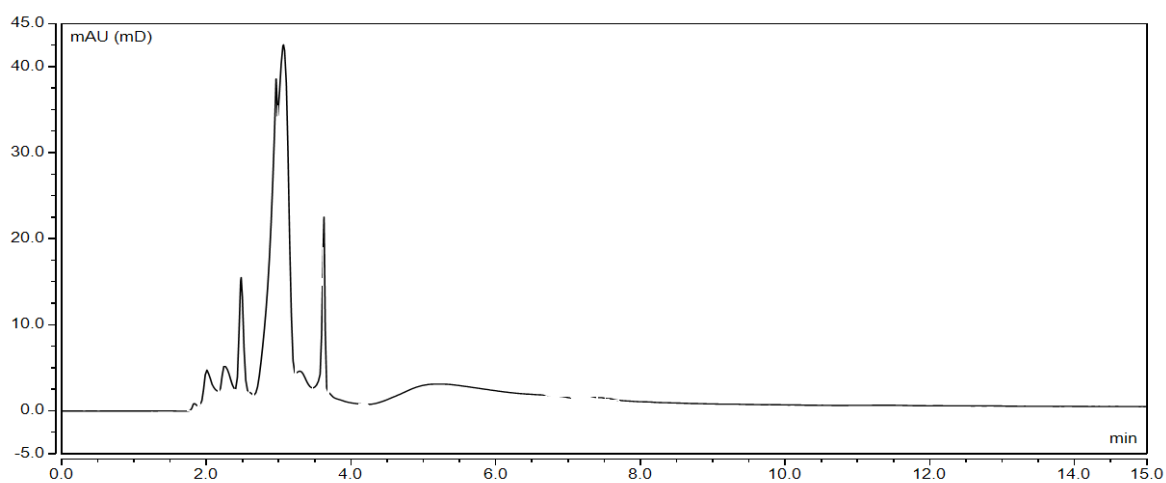


Figure S21. HPLC of H₄aPyta in the presence of Cu³⁺ ($t_r=2.482, 3.067$ min).

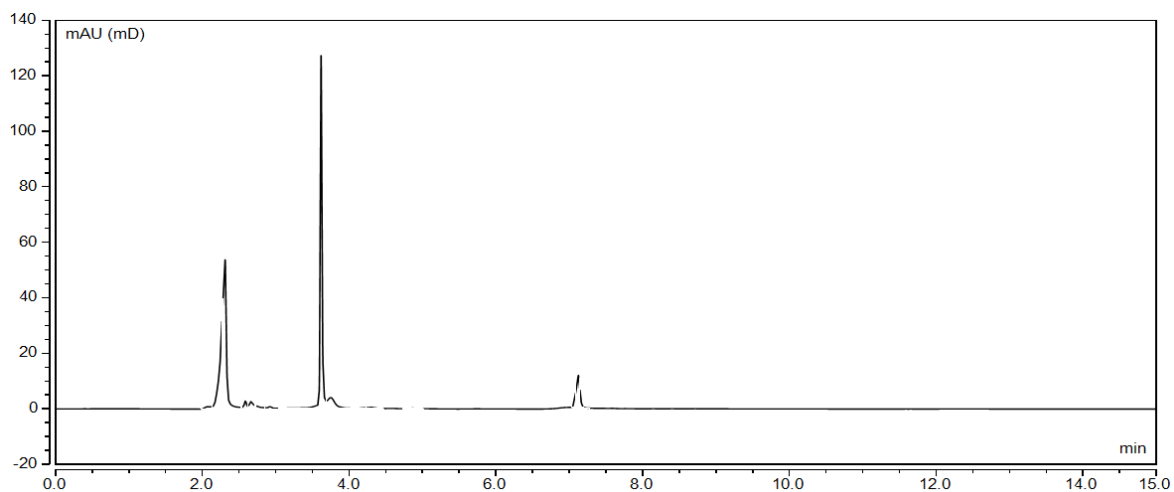


Figure S22. HPLC of H₄aPyta in the presence of Y³⁺ ($t_r=2.310$ min).

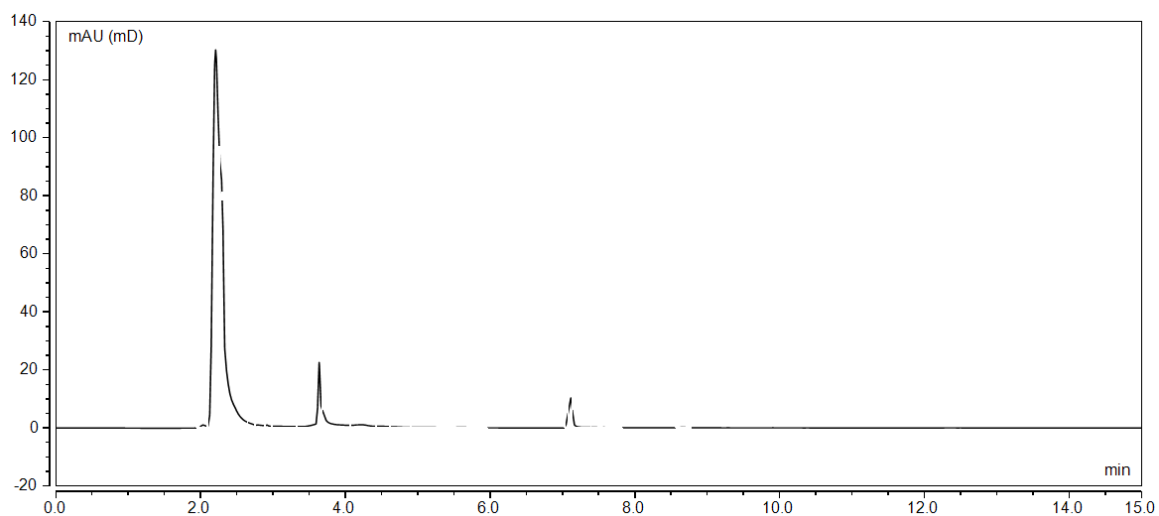


Figure S23. HPLC of H₄aPyta in the presence of Bi³⁺ ($t_r=2.208$ min).

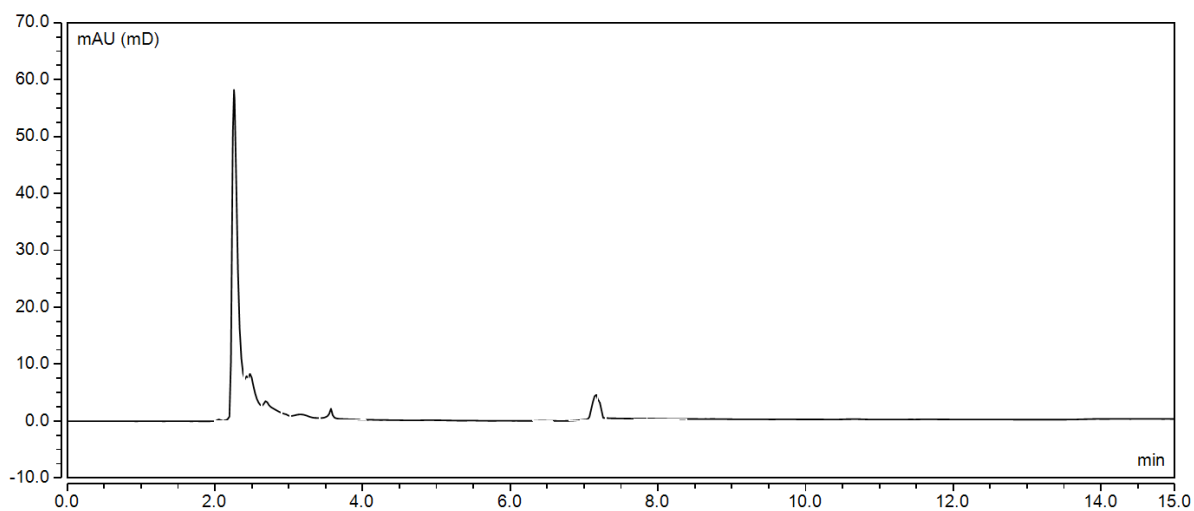


Figure S24. HPLC of H₆aPyha in the presence of Cu²⁺ ($t_r=2.260$ min).

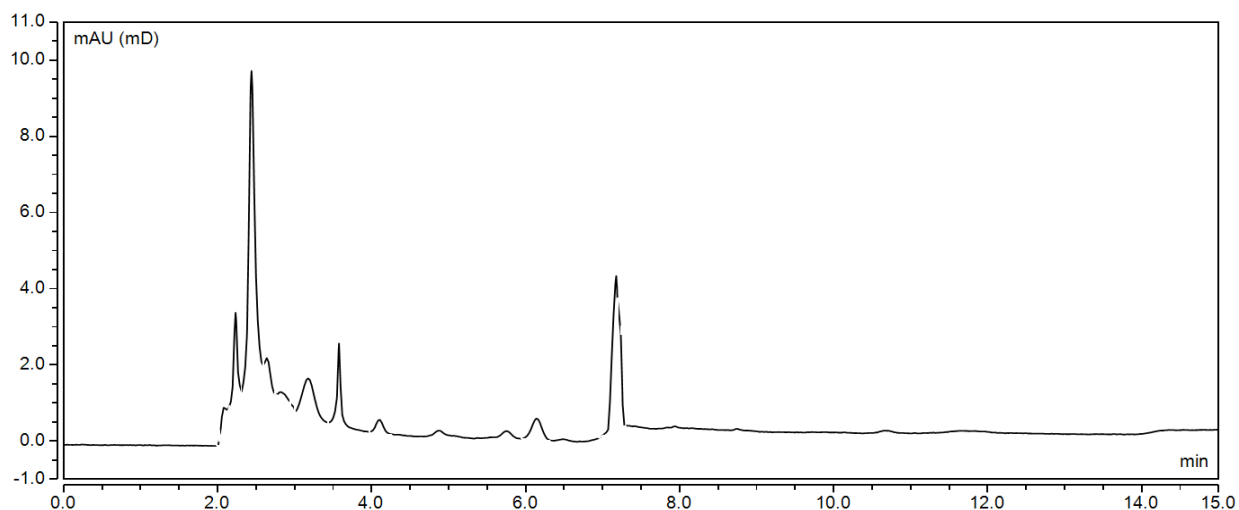


Figure S25. HPLC of H₆aPyha in the presence of Y³⁺ ($t_r=2.440$ min).

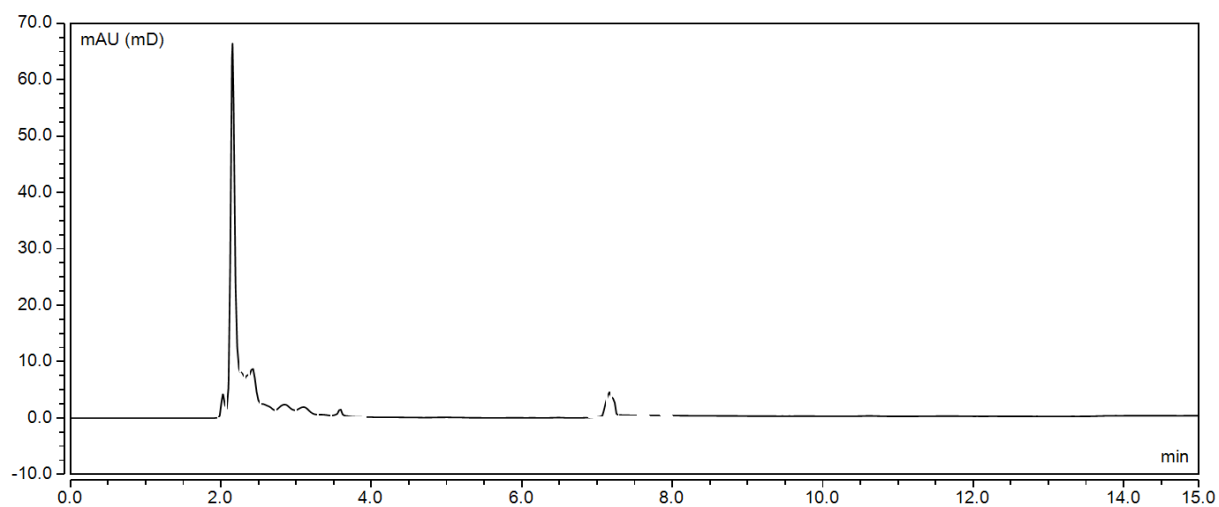


Figure S26. HPLC of H₆aPyha in the presence of Bi³⁺ ($t_r=2.155$ min).

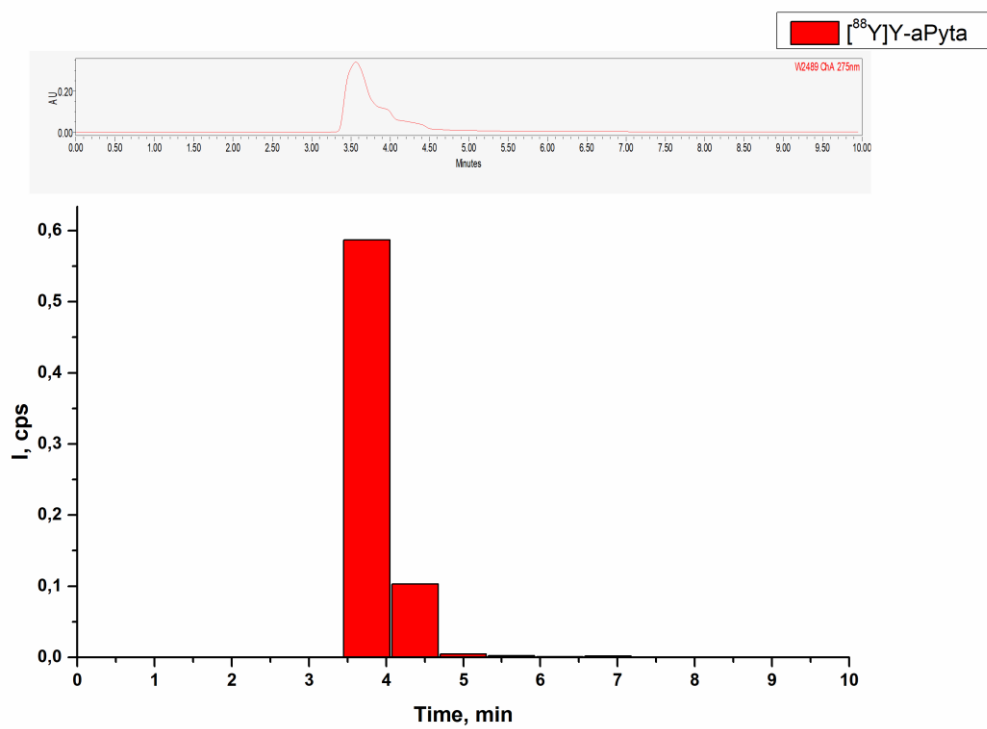


Figure S27. HPLC chromatogram obtained by UV-vis absorption detector and radioactivity measurements of H_4aPyta complexes with $[^{88}\text{Y}]\text{Y}^{3+}$.

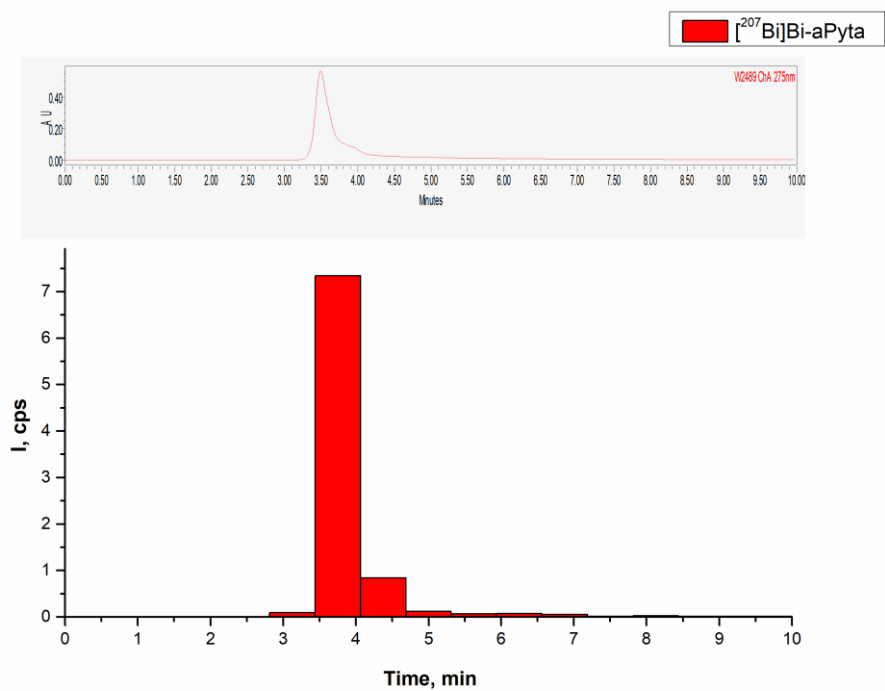


Figure S28. HPLC chromatogram obtained by UV-vis absorption detector and radioactivity measurements of H_4aPyta complexes with $[^{207}\text{Bi}]\text{Bi}^{3+}$.

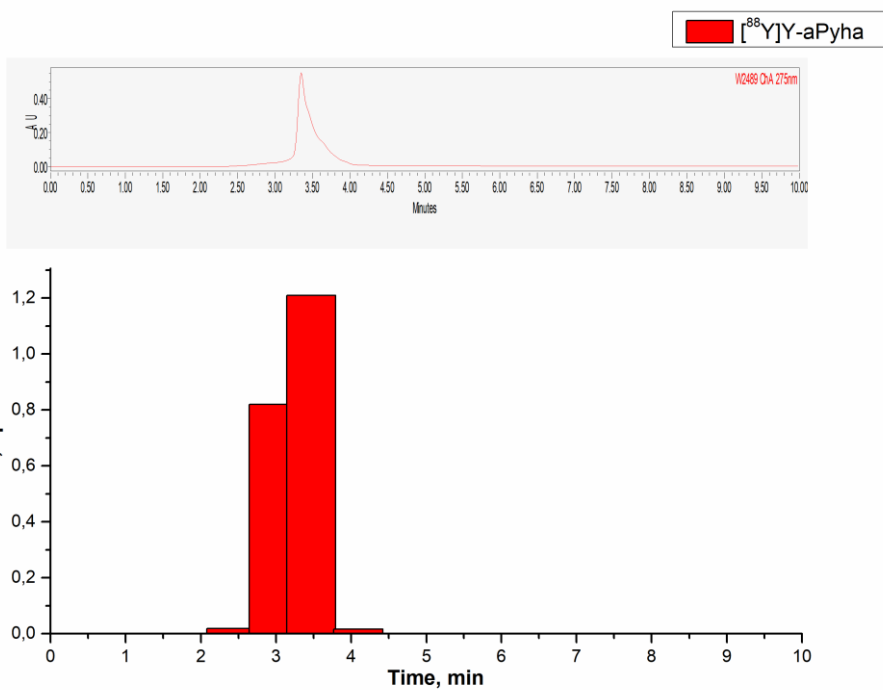


Figure S29. HPLC chromatograms obtained by UV-vis absorption detector and radioactivity measurements of H_6aPyha complexes with $[^{88}\text{Y}]\text{Y}^{3+}$.

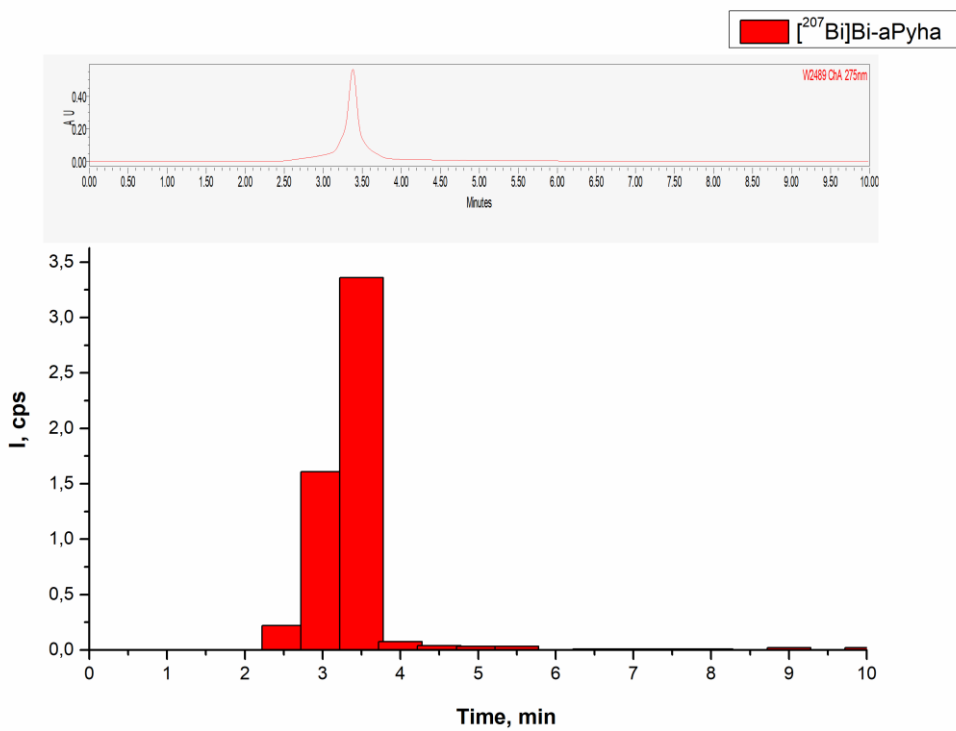


Figure S30. HPLC chromatograms obtained by UV-vis absorption detector and radioactivity measurements of H_6aPyha complexes with $[^{207}\text{Bi}]\text{Bi}^{3+}$.

5. DFT calculations

QTAIM analysis

We have performed a QTAIM analysis to investigate the Ga coordination in the **Ga-aPyta** complex. We may conclude the Ga ion is 6-coordinated with four oxygen and two nitrogen atoms (Table S3, Figure S31).

Table S3. The parameters of bond critical points (3,-1).

Bond	ρ	$\nabla^2\rho$	dH
Me-N	0.0381	0.0734	-0.0079
Me-N	0.0387	0.0716	-0.0079
Me-O	0.1000	0.4810	-0.0234
Me-O	0.1024	0.4951	-0.0251
Me-O	0.1000	0.4771	-0.0239
Me-O	0.0990	0.4732	-0.0230

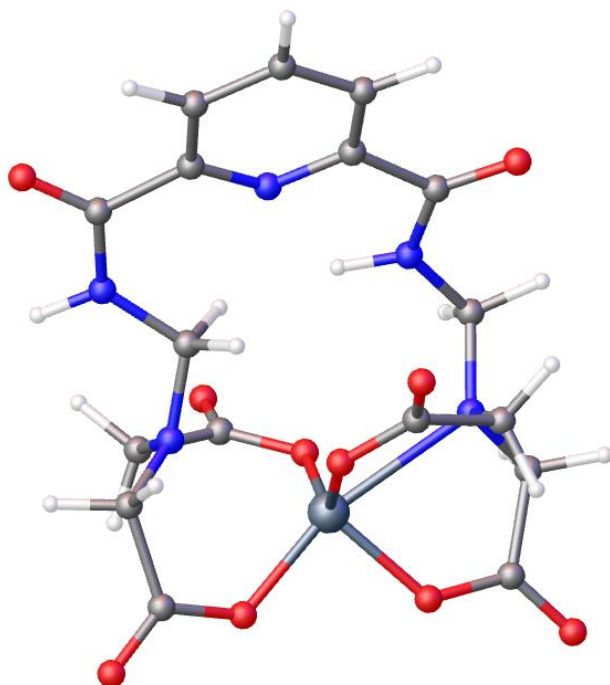


Figure S31. Geometries of complex **Ga-aPyta** calculated by the DFT method.

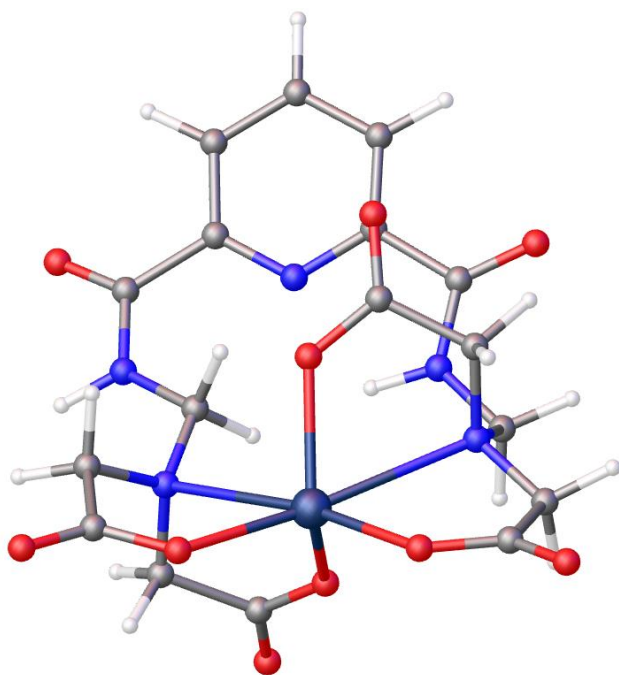


Figure S32. Geometries of complex **Y-aPyta** calculated by the DFT method.

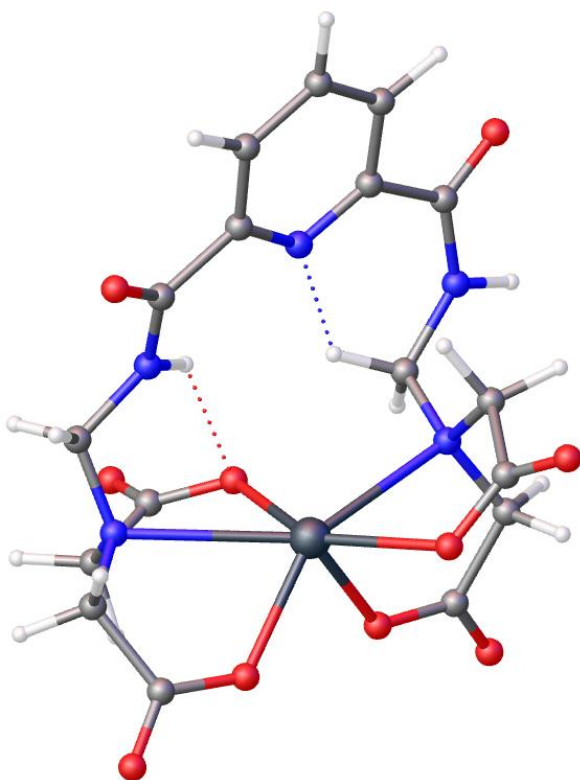


Figure S33. Geometries of complex **Bi-aPyta** calculated by the DFT method.

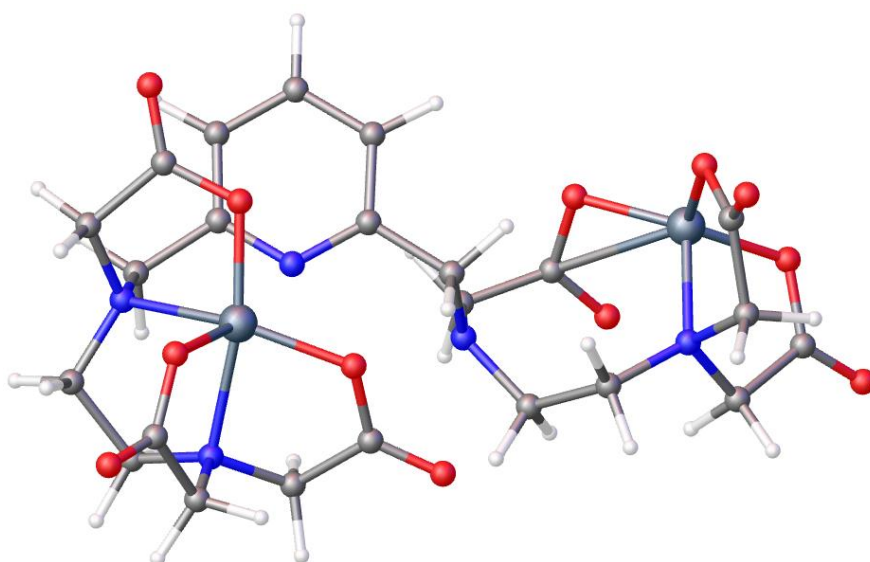


Figure S34. Geometries of complex **Ga₂-aPyha** calculated by the DFT method.

6. Radiolabeling

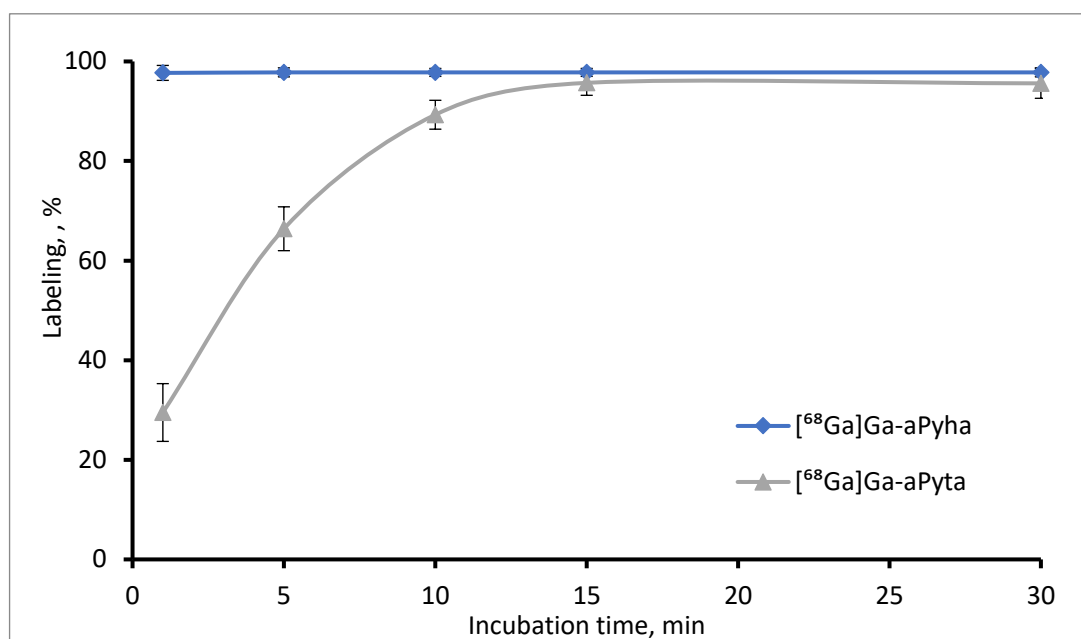


Figure S35. Time dependences of [⁶⁸Ga]Ga-aPyta and [⁶⁸Ga]Ga-aPyha formation (95°C, pH 5).

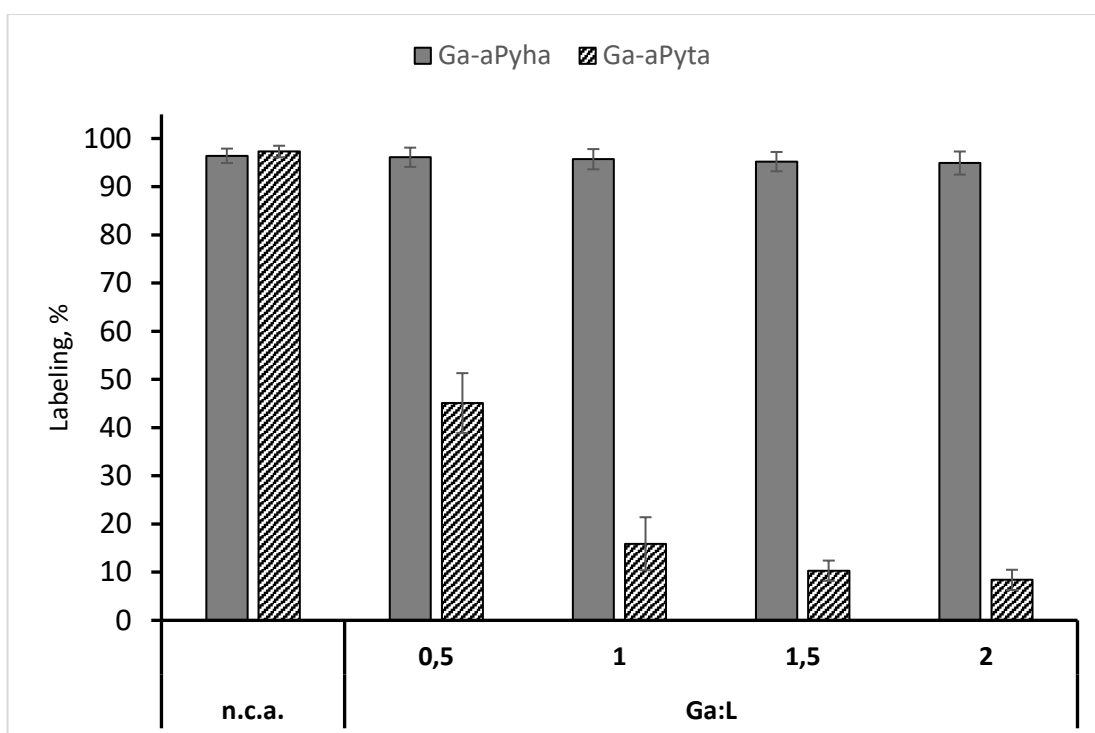


Figure S36. Influence of metal:ligand ratio on the yield of complexation reaction of H₄aPyta and H₆aPyha with ⁶⁸Ga (95°C, pH 5).

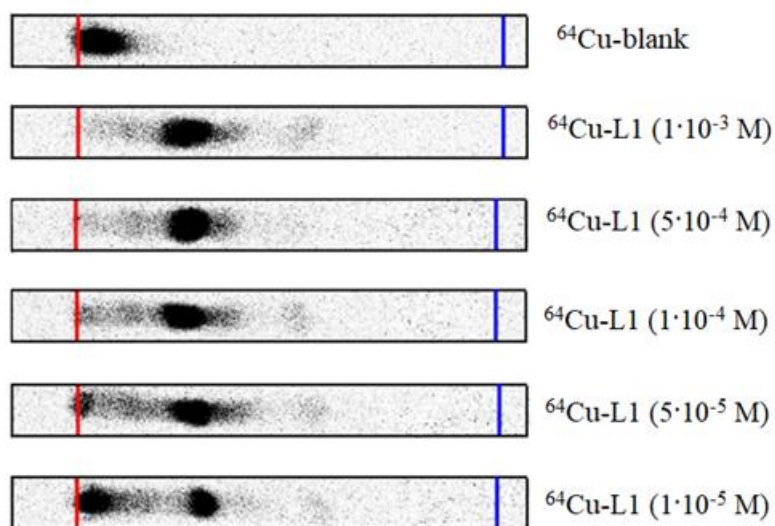


Figure S37. The image of TLC plates (Al-backed SiO₂ plates) after elution (20% NH₄Cl/MeOH =1/1) of ⁶⁴Cu complexes with H₆aPyha. Red – start line, blue – front line.

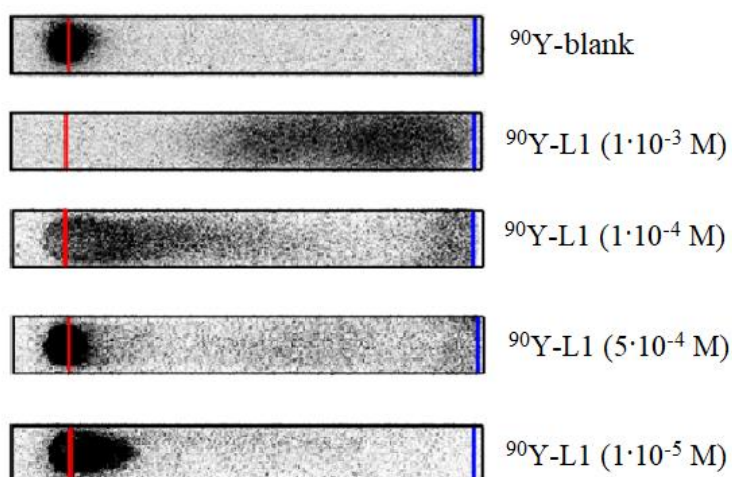


Figure S38. The image of “Whatman” sheets after elution (20% NH₄Cl/MeOH =3/7) of ⁹⁰Y complexes with H₆aPyha. Red – start line, blue – front line.

7. *In vitro* stability

Table S4. Stability of labelled **H₆aPyha** complex ²⁰⁷Bi in the presence of serum proteins.

Incubation time	Intact [²⁰⁷ Bi]Bi-aPyha complex, %
0 min	92,87356
30 min	84,53159
1 h	86,99552
2 h	85,7997
3 h	83,10912
4 h	90,58296
6 h	89,98505
1 d	97,3262
2 d	103,908
3 d	83,21839
4 d	90,55258
8 d	98,75223

8. Potentiometry

Table S5. Stepwise protonation constants (LogK) of the **aPyta⁴⁻** and **aPyha⁶⁻**.

Reaction equations	LogK
$\text{aPyta}^{4-} + \text{H}^+ \leftrightarrow \text{HaPyta}^{3-}$	9.19
$\text{HaPyta}^{3-} + \text{H}^+ \leftrightarrow \text{H}_2\text{aPyta}^{2-}$	7.9
$\text{H}_2\text{aPyta}^{2-} + \text{H}^+ \leftrightarrow \text{H}_3\text{aPyta}^-$	3.04
$\text{H}_3\text{aPyta}^- + \text{H}^+ \leftrightarrow \text{H}_4\text{aPyta}$	2.22
$\text{aPyha}^{6-} + \text{H}^+ \leftrightarrow \text{HaPyha}^{5-}$	10.16
$\text{HaPyha}^{5-} + \text{H}^+ \leftrightarrow \text{H}_2\text{aPyha}^{4-}$	9.36
$\text{H}_2\text{aPyha}^{4-} + \text{H}^+ \leftrightarrow \text{H}_3\text{aPyha}^{3-}$	5.87
$\text{H}_3\text{aPyha}^{3-} + \text{H}^+ \leftrightarrow \text{H}_4\text{aPyha}^{2-}$	4.57
$\text{H}_4\text{aPyha}^{2-} + \text{H}^+ \leftrightarrow \text{H}_5\text{aPyha}^-$	3.22
$\text{H}_5\text{aPyha}^- + \text{H}^+ \leftrightarrow \text{H}_6\text{aPyha}$	1.88

Table S6. Hydrolysis constants of Cu^{2+} , Y^{3+} , Ga^{3+} and Bi^{3+} ions used to calculate the total binding constants of the **aPyta⁴⁻** and **aPyha⁶⁻** complexes with Cu^{2+} , Y^{3+} , Ga^{3+} and Bi^{3+} in the Hyperquad2003 program.

Reaction equations	$\text{M}^{n+} =$			
	Cu^{2+}	Y^{3+}	Ga^{3+}	Bi^{3+}
$\text{M}^{n+} + \text{H}_2\text{O} \leftrightarrow \text{MOH}^{(n-1)} + \text{H}^+$	-7.97[c]	-7.7[a]	-2.6[b]	-1.09[a]
$\text{M}^{n+} + 2\text{H}_2\text{O} \leftrightarrow \text{M}(\text{OH})_2^{(n-2)} + 2\text{H}^+$	-16.23[c]	-16.4[a]	-5.9[b]	-4.0[a]
$\text{M}^{n+} + 3\text{H}_2\text{O} \leftrightarrow \text{M}(\text{OH})_3^{(n-3)} + 3\text{H}^+$	-26.6[b]	-26.0[a]	-10.3[b]	-8.86[a]
$\text{M}^{n+} + 4\text{H}_2\text{O} \leftrightarrow \text{M}(\text{OH})_4^{(n-4)} + 4\text{H}^+$	-39.7[b]	-36.5[a]	-16.6[b]	-21.8[a]
$2\text{M}^{n+} + \text{H}_2\text{O} \leftrightarrow \text{M}_2\text{OH}^{(2n-1)} + \text{H}^+$	-6.71[c]	-	-	-
$6\text{M}^{n+} + 12\text{H}_2\text{O} \leftrightarrow \text{M}_4(\text{OH})_4^{(6n-12)} + 12\text{H}^+$	-	-	-	-1.0[b]
$2\text{M}^{n+} + 2\text{H}_2\text{O} \leftrightarrow \text{M}_2(\text{OH})_2^{(2n-2)} + 2\text{H}^+$	-10.55[c]	-14.23[a]	-	-
$3\text{M}^{n+} + 4\text{H}_2\text{O} \leftrightarrow \text{M}_3(\text{OH})_4^{(3n-4)} + 4\text{H}^+$	-20.95[c]	-	-	-
$3\text{M}^{n+} + 5\text{H}_2\text{O} \leftrightarrow \text{M}_2(\text{OH})_6^{(3n-5)} + 5\text{H}^+$	-	-31.6[a]	-	-
$26\text{M}^{n+} + 65\text{H}_2\text{O} \leftrightarrow \text{M}_{26}(\text{OH})_{65}^{(26n-65)} + 65\text{H}^+$	-	-	-139.1[b]	-

[a] Baes, C.F. and Mesmer, R.E. "The Hydrolysis of Cations", John Wiley & Sons, Inc., New York, 1976, P. 489.

[b] Paul L. Brown and Christian Ekberg, "Hydrolysis of Metal Ions", Wiley-VCH, 2016, V.2, P.917.

[c] Natalia V. Plyasunova, Mingsheng Wang, Yu Zhang, Mamoun Muhammed, Critical evaluation of thermodynamics of complex formation of metal ions in aqueous solutions II. Hydrolysis and hydroxo-complexes of Cu^{2+} at 298.15 K, Hydrometallurgy, 1997, 45, 37-51.

Table S7. Stepwise binding constants of protonated **aPyta⁴⁻** and **aPyha⁶⁻** with **Cu²⁺**, **Y³⁺**, **Ga³⁺** and **Bi³⁺** ions.

Reaction equations	logK			
	Cu ²⁺	Y ³⁺	Ga ³⁺	Bi ³⁺
$\text{aPyta}^{4-} + \text{M}^{n+} \leftrightarrow \text{MaPyta}^{n-4}$	14.96	8.9	19.5	28.78
$\text{HaPyta}^{3-} + \text{M}^{n+} \leftrightarrow \text{MHaPyta}^{n-3}$	11.31	6.89	14.21	26.25
$\text{H}_2\text{aPyta}^{2-} + \text{M}^{n+} \leftrightarrow \text{MH}_2\text{aPyta}^{n-2}$		3.54		
$\text{aPyha}^{6-} + \text{M}^{n+} \leftrightarrow \text{MaPyha}^{n-6}$	-	15.05	27.38	-
$\text{HaPyha}^{5-} + \text{M}^{n+} \leftrightarrow \text{MHaPyha}^{n-5}$	18.21	13.23	-	
$\text{H}_2\text{aPyha}^{4-} + \text{M}^{n+} \leftrightarrow \text{MH}_2\text{aPyha}^{n-4}$	11.38	8.7	-	-
$\text{H}_3\text{aPyha}^{3-} + \text{M}^{n+} \leftrightarrow \text{H}_3\text{MaPyha}^{n-3}$		5.77	19.81	-

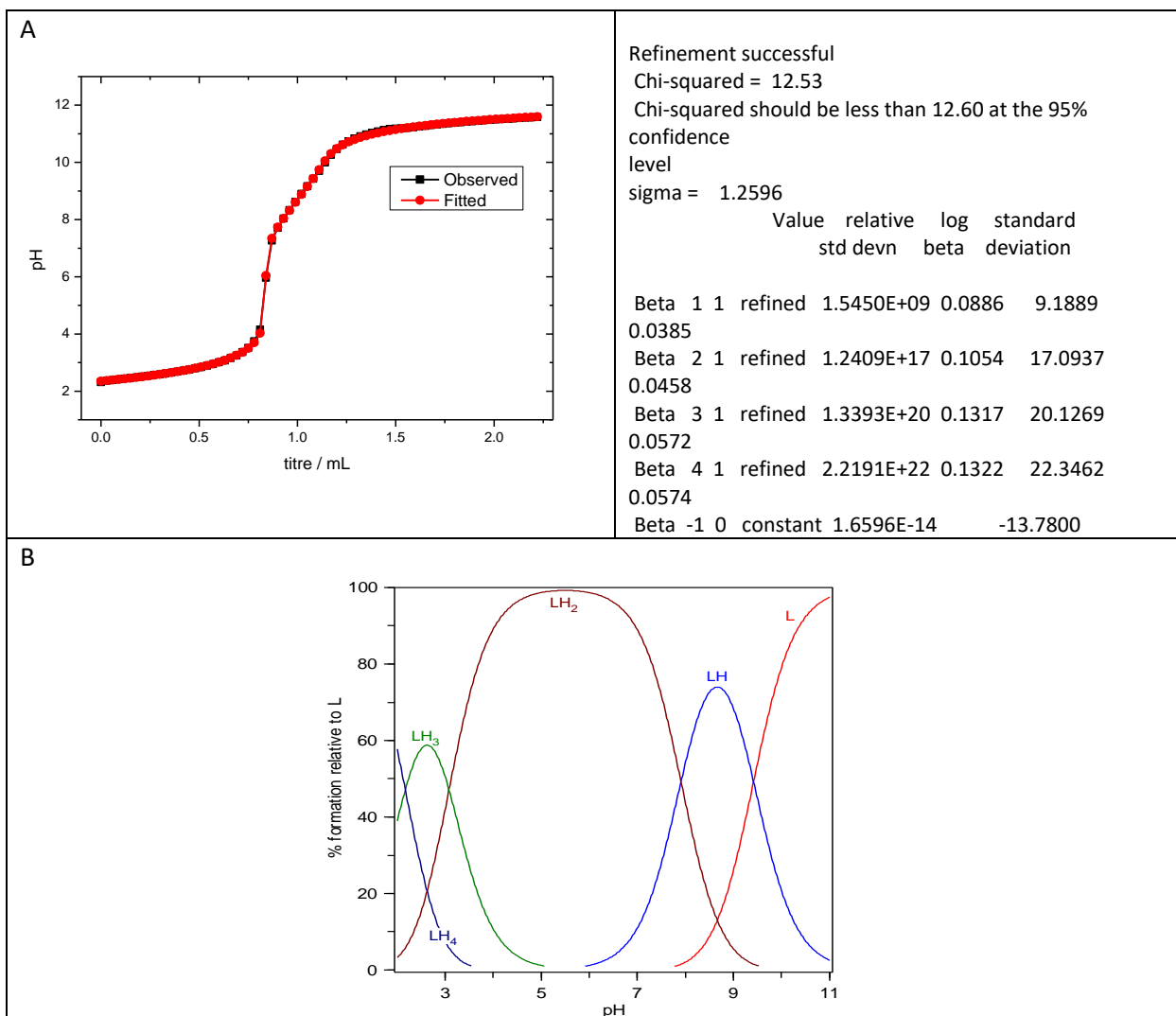


Figure S39. Potentiometric titration curves observed (black points) and fitted (red points) and statistical parameters obtained by the HYPERQUAD2003 program (A), and ligand **aPyta**⁴⁻ (1 mM) species distribution as a function of pH (B).

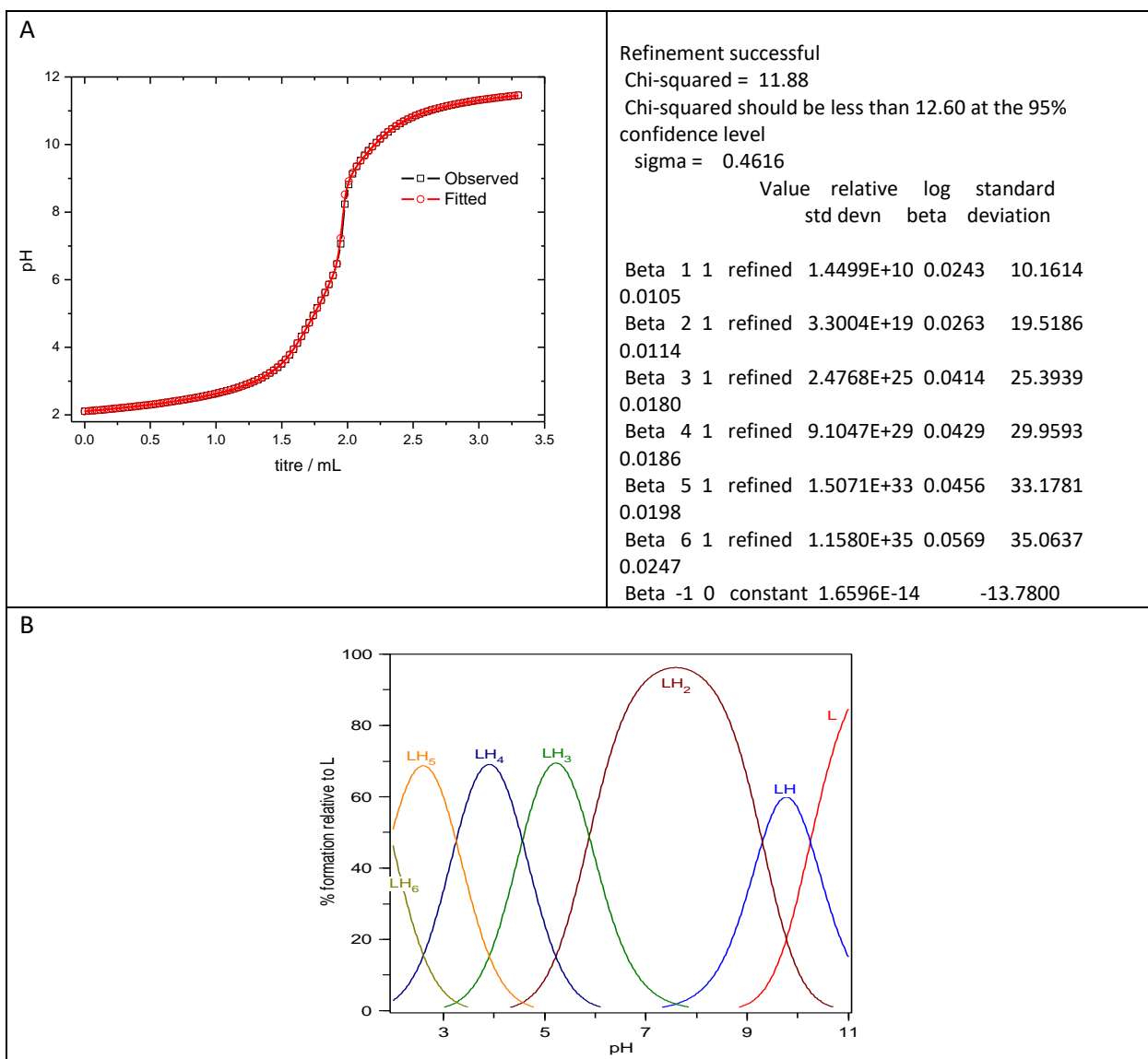


Figure S40. Potentiometric titration curves observed (black points) and fitted (red points) and statistical parameters obtained by the HYPERQUAD2003 program (A), and ligand **aPyha**⁶⁻ (1 mM) species distribution as a function of pH (B).

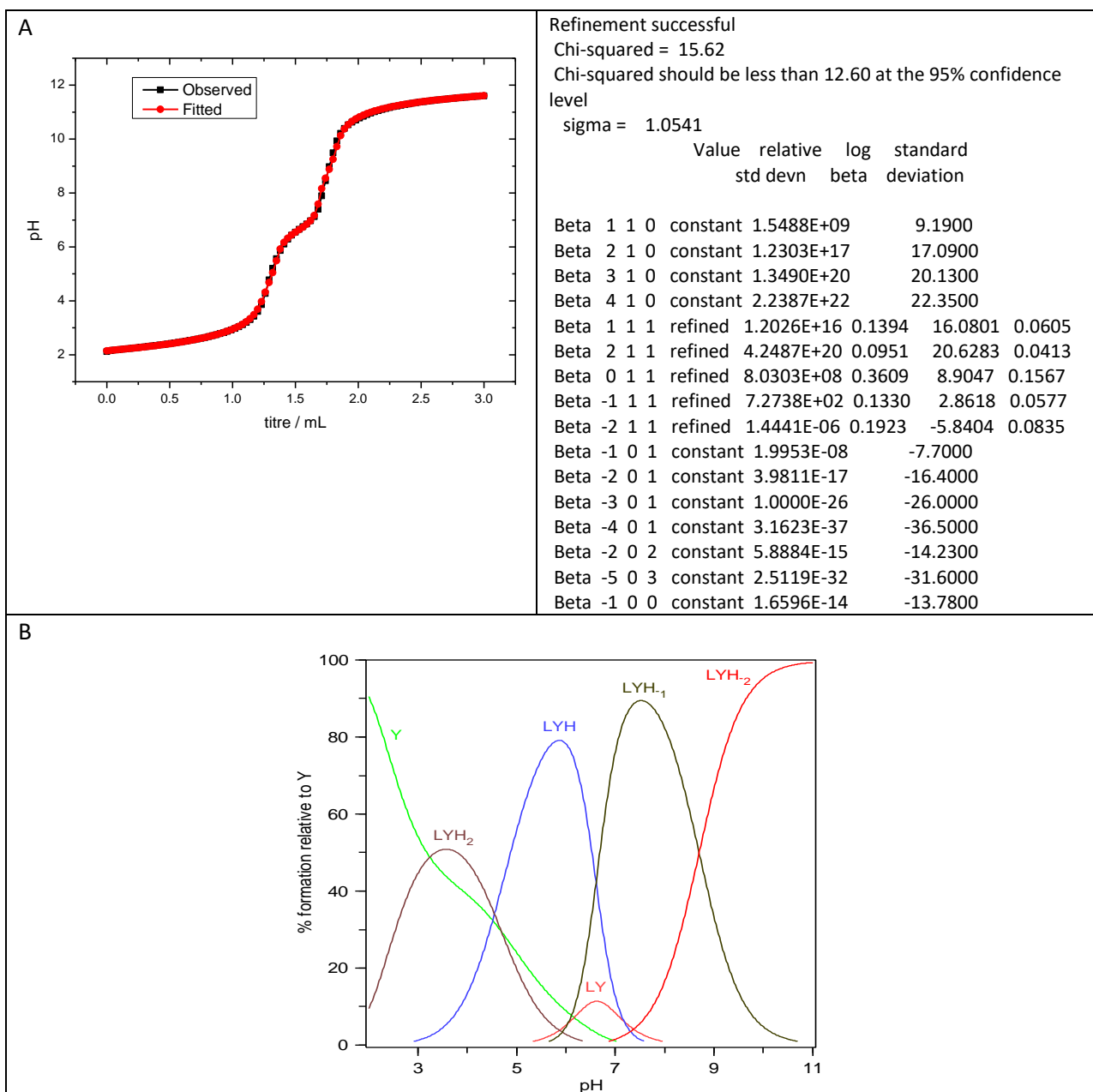


Figure S41. Potentiometric titration curves observed (black points) and fitted (red points) and statistical parameters obtained by the HYPERQUAD2003 program (A), and species distribution diagram in the system Y^{3+} (1 mM), $aPyta^{4-}$ (1 mM), KNO_3 (0.1 M) as a function of pH (B).

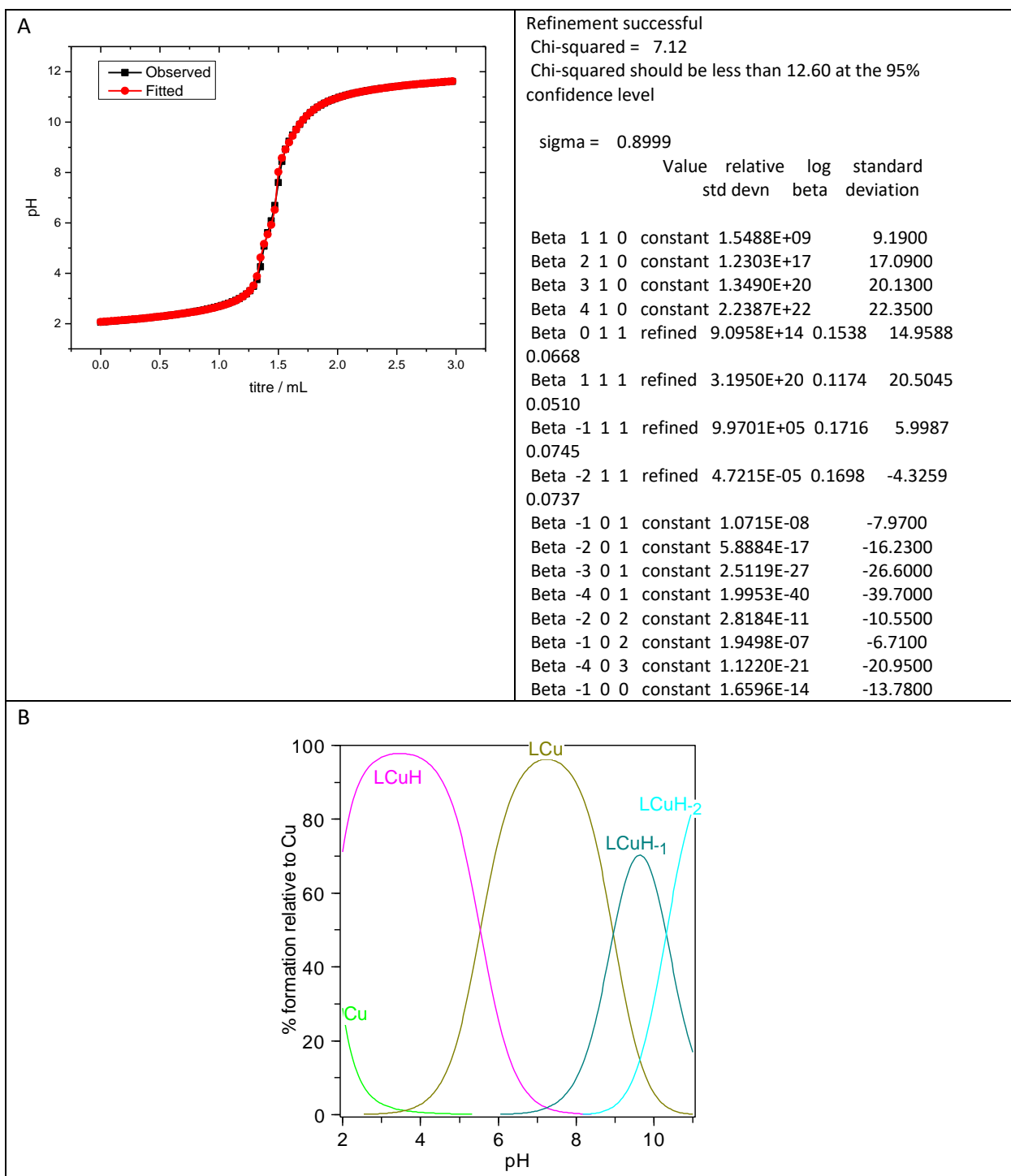


Figure S42. Potentiometric titration curves observed (black points) and fitted (red points) and statistical parameters obtained by the HYPERQUAD2003 program (A), and species distribution diagram in the system Cu^{2+} (1 mM), aPyta^{4-} (1 mM), KNO_3 (0.1 M) as a function of pH (B).

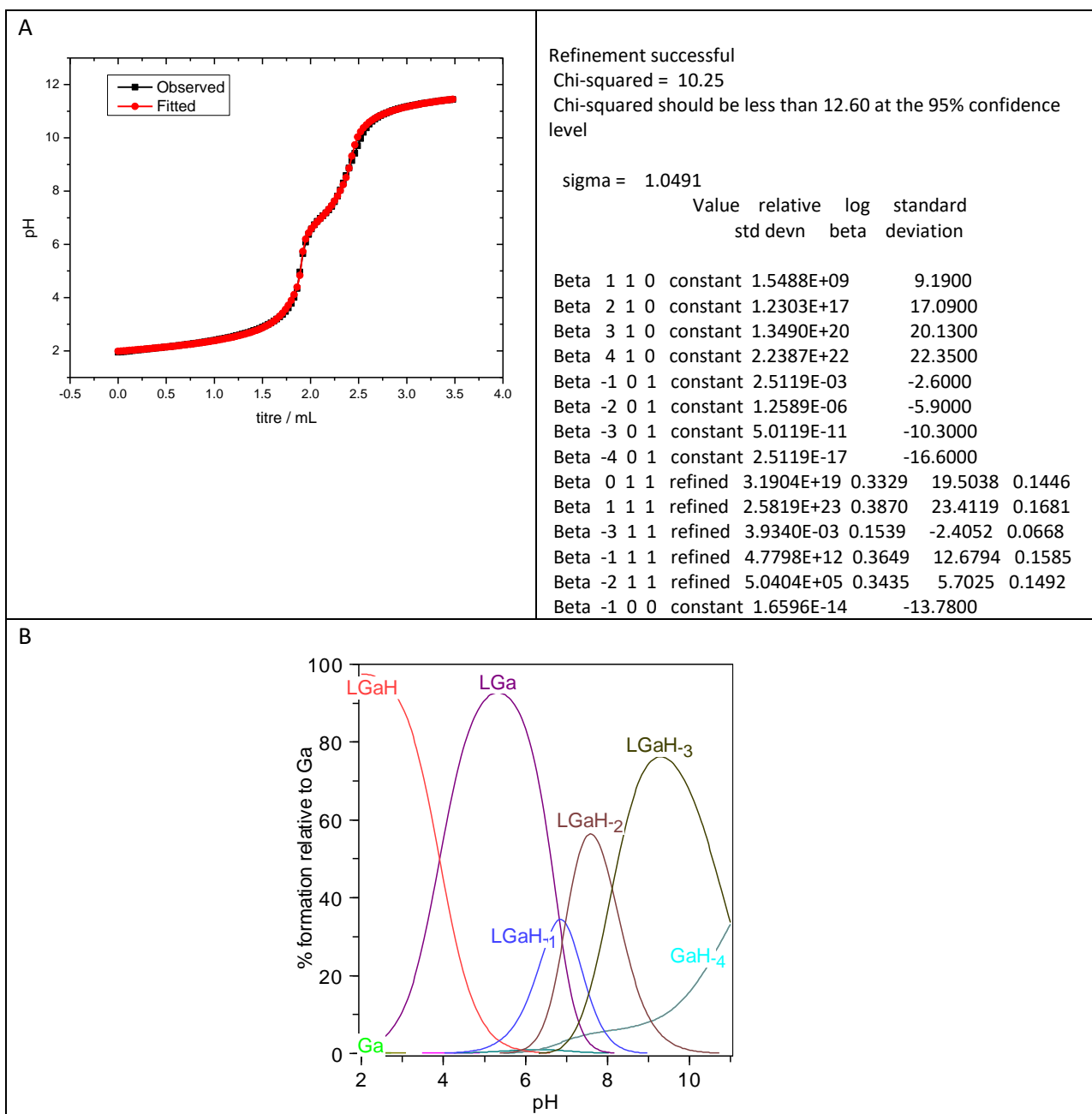


Figure S43. Potentiometric titration curves observed (black points) and fitted (red points) and statistical parameters obtained by the HYPERQUAD2003 program (A), and species distribution diagram in the system Ga^{3+} (1 mM), aPyta^{4-} (1 mM), KNO_3 (0.1 M) as a function of pH (B).

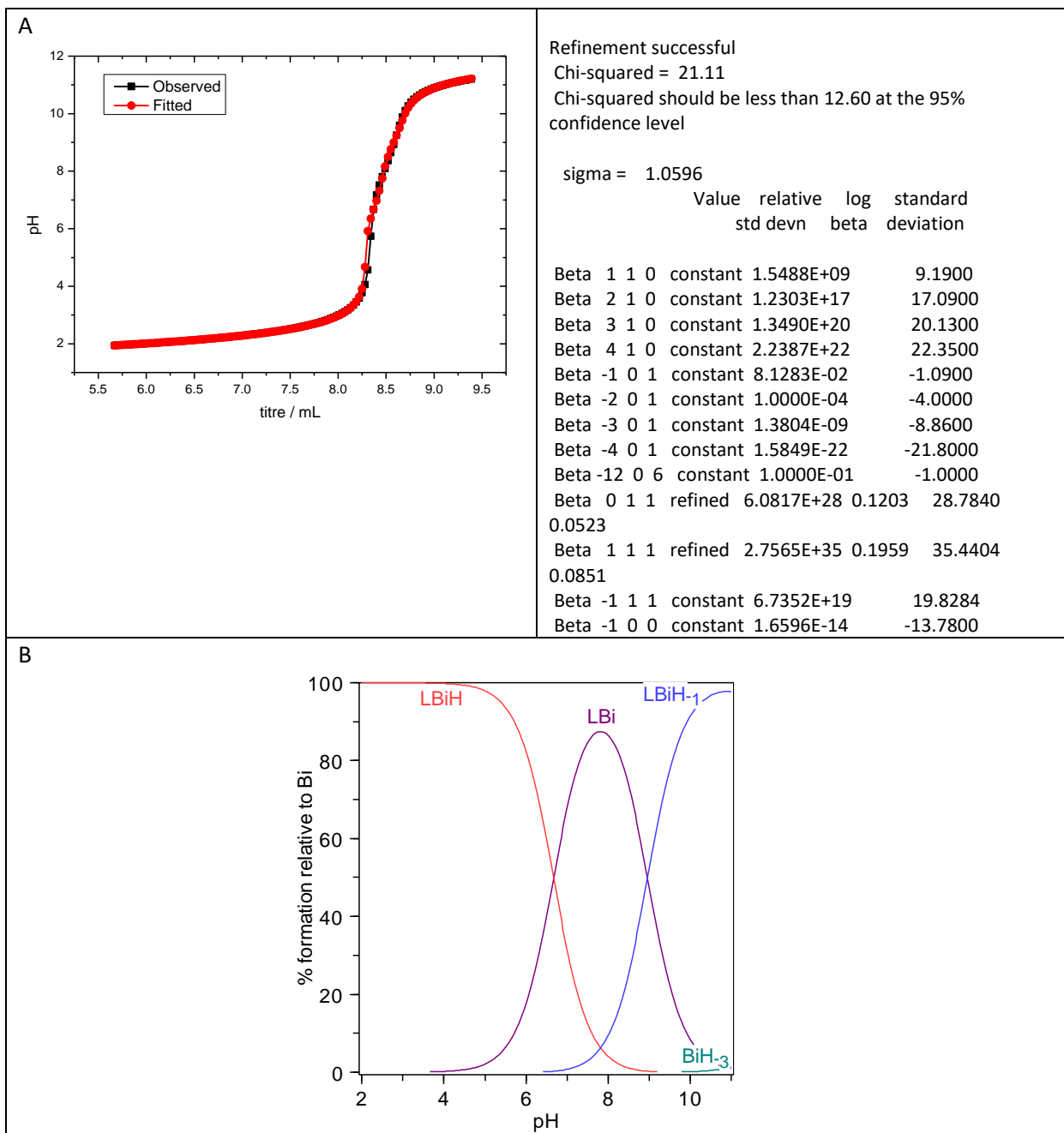


Figure S44. Potentiometric titration curves observed (black points) and fitted (red points) and statistical parameters obtained by the HYPERQUAD2003 program (A), and species distribution diagram in the system Bi^{3+} (1 mM), aPyta^{4-} (1 mM), KNO_3 (0.1 M) as a function of pH (B).

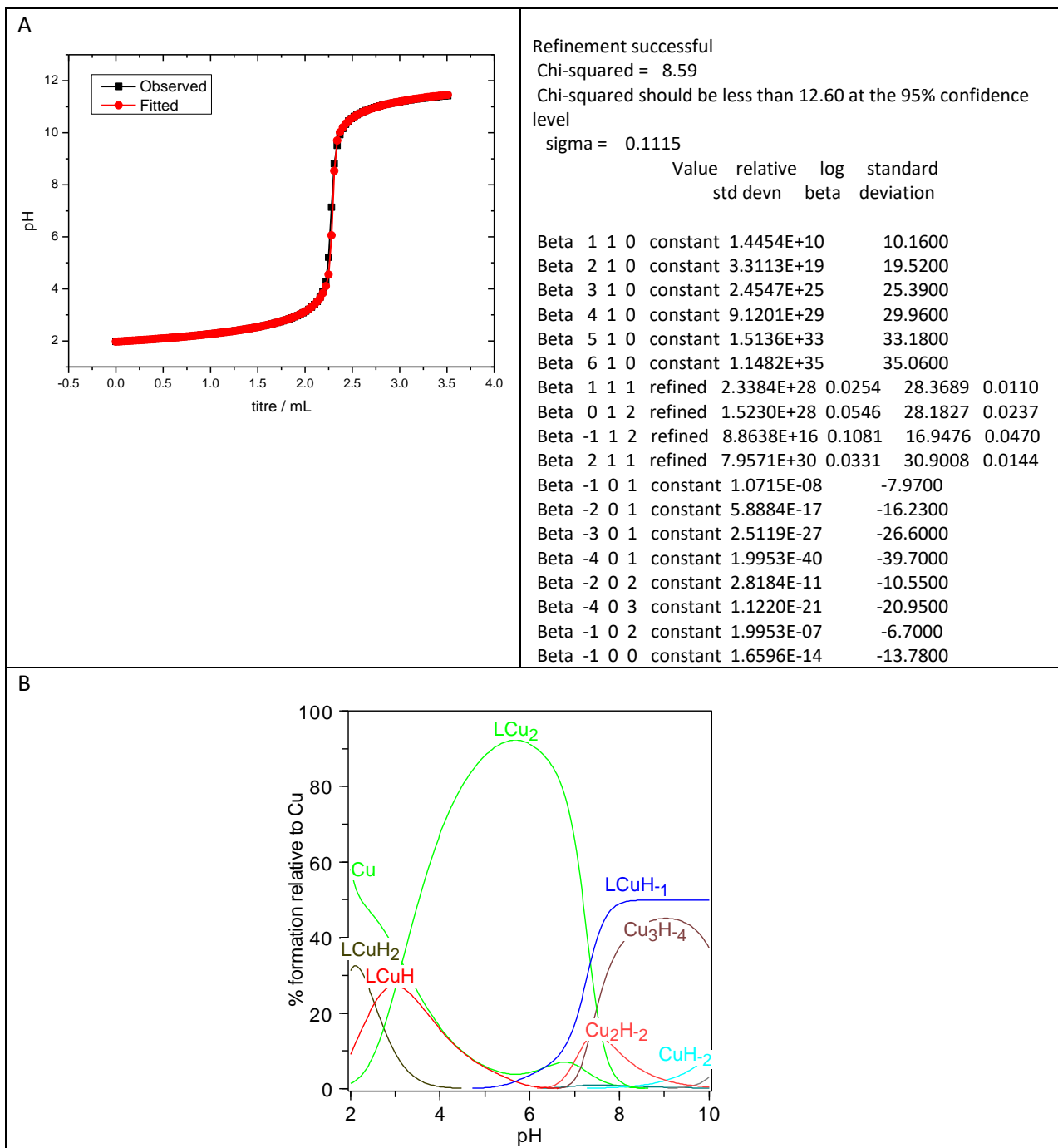


Figure S45. Potentiometric titration curves observed (black points) and fitted (red points) and statistical parameters obtained by the HYPERQUAD2003 program (A), and species distribution diagram in the system Cu^{2+} (2 mM), aPyha^{6-} (1 mM), KNO_3 (0.1 M) as a function of pH (B).

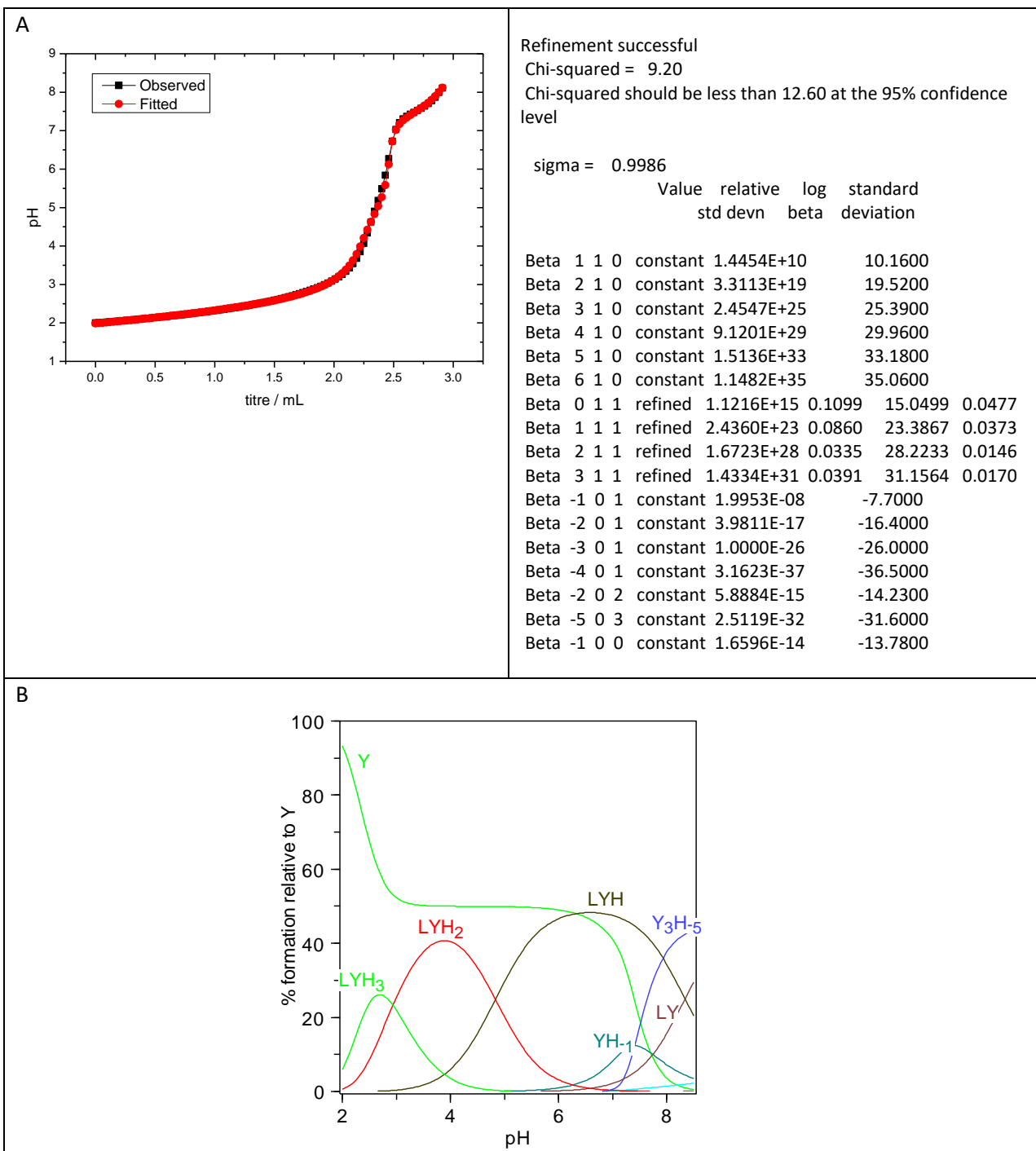


Figure S46. Potentiometric titration curves observed (black points) and fitted (red points) and statistical parameters obtained by the HYPERQUAD2003 program (A), and species distribution diagram in the system Y^{3+} (3.2 mM), $aPyha^{6-}$ (1.6 mM), KNO_3 (0.1 M) as a function of pH (B).

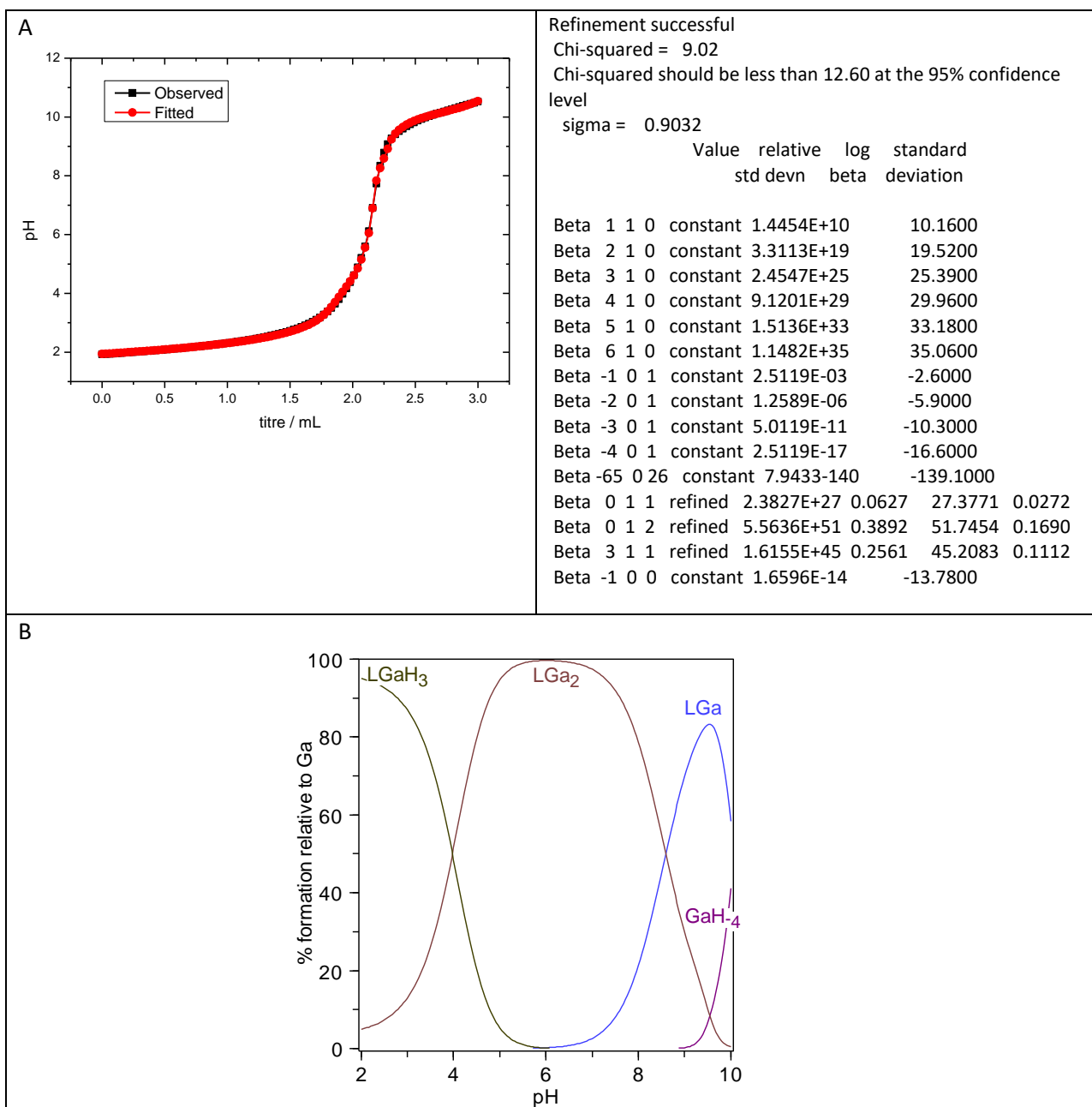


Figure S47. Potentiometric titration curves observed (black points) and fitted (red points) and statistical parameters obtained by the HYPERQUAD2003 program (A), and species distribution diagram in the system Ga^{3+} (1 mM), aPyha^{6-} (1 mM), KNO_3 (0.1 M) as a function of pH (B).

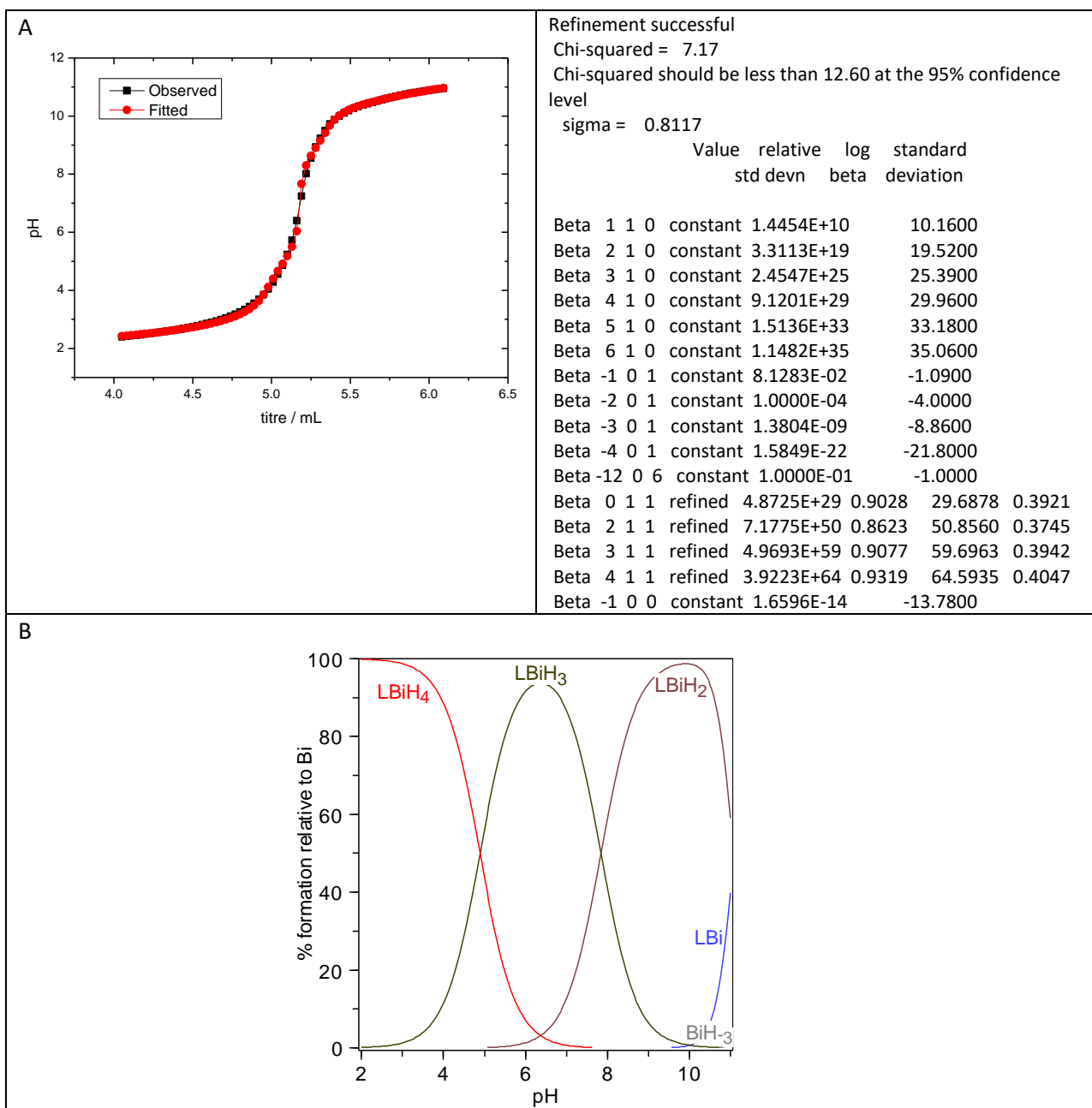


Figure S48. Potentiometric titration curves observed (black points) and fitted (red points) and statistical parameters obtained by the HYPERQUAD2003 program (A), and species distribution diagram in the system Bi^{3+} (0.9 mM), aPyha^{6-} (1 mM), KNO_3 (0.1 M) as a function of pH (B).

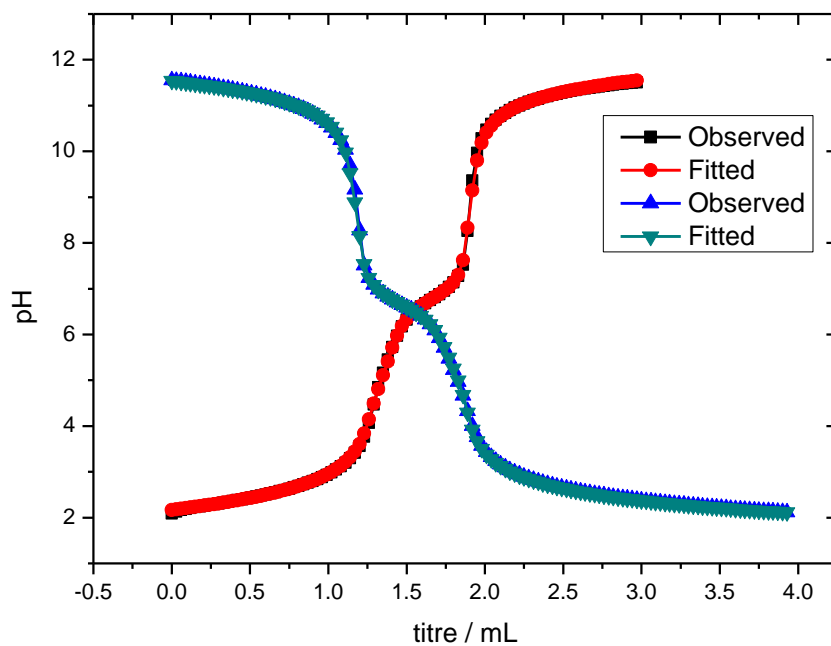


Figure S49. Potentiometric titration curves for direct titration observed (black points) and fitted (red points) and for back titration observed (blue points) and fitted (teal points) in the system Y^{3+} (1 mM), $aPyta^{4-}$ (1.3 mM), KNO_3 (0.1 M).

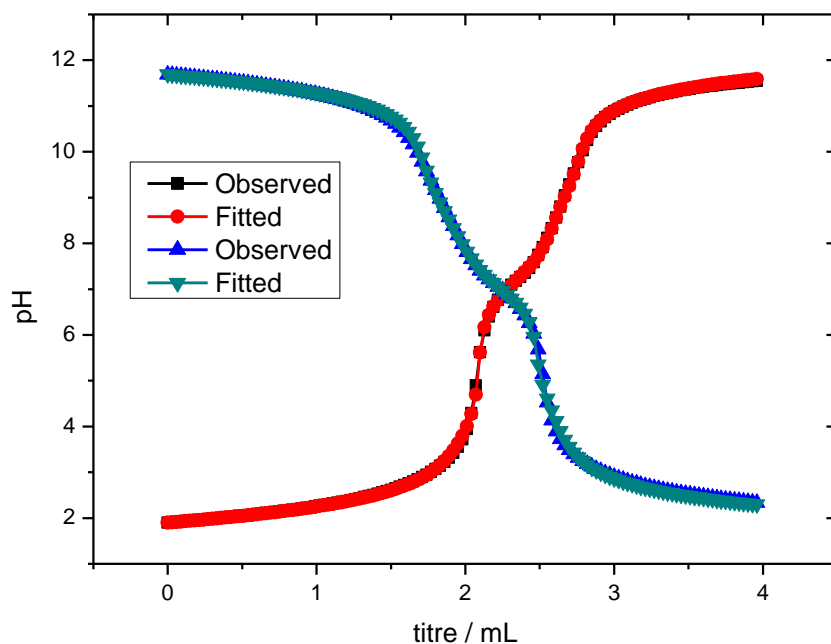


Figure S50. Potentiometric titration curves for direct titration observed (black points) and fitted (red points) and for back titration observed (blue points) and fitted (teal points) in the system Ga^{3+} (1 mM), $aPyta^{4-}$ (1.3 mM), KNO_3 (0.1 M).